Modeling the Formation and Vertical Mixing of Oil Droplets and Oil-Mineral Aggregates (OMAs) Under Breaking Wave Conditions

Tian Shen

A Thesis

in

The Department

of

Building, Civil and Environmental Engineering

Presented in Partial Fulfillment of the Requirements for the Degree of

Master of Applied Science (Civil Engineering) at

Concordia University

Montreal, Quebec, Canada

January 2010

Library and Archives
Canada

Published Heritage
Branch

395 Wellington Street
Ottawa ON K1A 0N4
Canada

Bibliothèque et
Archives Canada

Direction du
Patrimoine de l'édition

395, rue Wellington
Ottawa ON K1A 0N4
Canada

Your file Votre référence
ISBN: 978-0-494-67244-0
Our file Notre référence
ISBN: 978-0-494-67244-0

NOTICE:

The author has granted a non-exclusive license allowing Library and Archives Canada to reproduce, publish, archive, preserve, conserve, communicate to the public by telecommunication or on the Internet, loan, distribute and sell theses worldwide, for commercial or non-commercial purposes, in microform, paper, electronic and/or any other formats.

The author retains copyright ownership and moral rights in this thesis. Neither the thesis nor substantial extracts from it may be printed or otherwise reproduced without the author's permission.

AVIS:

L'auteur a accordé une licence non exclusive permettant à la Bibliothèque et Archives Canada de reproduire, publier, archiver, sauvegarder, conserver, transmettre au public par télécommunication ou par l'Internet, prêter, distribuer et vendre des thèses partout dans le monde, à des fins commerciales ou autres, sur support microforme, papier, électronique et/ou autres formats.

L'auteur conserve la propriété du droit d'auteur et des droits moraux qui protège cette thèse. Ni la thèse ni des extraits substantiels de celle-ci ne doivent être imprimés ou autrement reproduits sans son autorisation.

In compliance with the Canadian Privacy Act some supporting forms may have been removed from this thesis.

While these forms may be included in the document page count, their removal does not represent any loss of content from the thesis.

Conformément à la loi canadienne sur la protection de la vie privée, quelques formulaires secondaires ont été enlevés de cette thèse.

Bien que ces formulaires aient inclus dans la pagination, il n'y aura aucun contenu manquant.

Canada

Abstract

Modeling the Formation and Vertical Mixing of Oil Droplets and Oil-Mineral Aggregates (OMAs) Under Breaking Wave Conditions

Tian Shen

Cleanup of oil spills, especially at the shoreline, is confronted with challenging problems of both technology and cost-effectiveness. Over the past decades, a new hypothesis has emerged, that the formation of Oil-Mineral Aggregates (OMAs) consisting of oil droplets and mineral fines, enhances the dispersion of oil in aquatic environments. Despite its documented role in cleaning oil spills along shorelines through reported experimental studies, the literature on the mathematical modeling of the formation and dispersion of OMAs has been limited.

In the present study, the physical processes were investigated including oil slick breaking up under breaking wave, the formation of OMAs, and oil/OMAs vertical mixing. A modeling approach was developed for simulating the formation and vertical mixing of oil droplets and OMAs, namely Oil Droplet and OMAs Simulation (OMA-SIM). This method integrated modeling tools for addressing the oil vertical mixing model and density based OMAs formation model to examine the dispersion of oil droplets and OMAs.

The OMA-SIM was validated using data obtained from mesoscale wave tank experiments. The concentration and size of oil droplets and OMAs generated under breaking wave condition were simulated and compared with experimental data. The main factors that affect oil droplets and OMAs formation and vertical mixing have been studied and concerned in the developed model. These factors include oil density and viscosity, oil/water interfacial tension, wave energy dispersion rate, dispersants, and environment temperature. The results of the case studies suggest that the OMA-SIM developed in this study provide effective methods for simulating and predicting the vertical dispersion of spilled oil. A computation system was then developed that couples the OMA-SIM with a user-friendly interface system, and the system was applied to real case studies based on field data.

OMA-SIM results indicated that the energy dissipation rate of breaking waves is the predominant factor which affects the concentration and particle size of oil droplets and OMAs. The higher the breaking wave energy, the more oil was dispersed with time after the experimental oil spill. Oil viscosity has a significant influence on dispersed oil concentration. The mass of dispersed oil decreased with increasing oil viscosity. Increasing temperature to decrease oil viscosity and then to enhance the formation of OMAs resulted in a greater concentration of oil. The dispersants reduce oil/water interfacial tension and result in a decreased size of oil droplets and OMAs. The application of mineral fines facilitates the formation of OMAs.

ACKNOWLEDGEMENTS

My deepest thanks go to my supervisor, Dr. Zhi Chen, for his persistence and guidance of my research studies. I would like to thank Dr. Kenneth Lee who provided experimental data for our modeling system.

I am grateful to Lin Zhao, Jin Yuan, and Niema Afroze for their friendship and support. Our many discussions resulted in practical advancement in the development of the model. I would also like to thank all the stuff at Department of Building, Civil, and Environmental Engineering of Concordia University for providing me a helpful environment to accomplish my study.

Many thanks go to my parents Tianyu Shen and Yumin Xia and my sisters Yan Shen and Hua Shen for their enduring love, patience, and support over last few years. In particular, my wife Yueli Wang was unquestioning in her understanding and support.

Table of Contents

Chapter 5: Model Applications and Further Examination of the Key Model Parameters through Four Case Analyses....62

Chapter 6: Thesis Contribution and Conclusion....85

List of Figures

List of Tables

List of Symbols

ε	Wave energy dissipation rate (m^2 s^{-3})
h	Water depth (m)
H_b	Breaking wave height (m)
H_{rms}	Root mean square wave height (m)
H_m	Maximum possible wave height (m)
L	Wave length (m)
T	Wave period
ω	Wave frequency
c_g	Wave group velocity (m s^{-1})
C	Wave velocity (m s^{-1})
Q_b	Fraction of the total number of waves
$F(h)$	Probability distribution of wave heights
r_{max}	Maximum radius of oil droplet (m)
$r_{\min}$	Minimum droplet radius (m)
ν_o	Kinematic viscosity of the oil (m^2 s^{-1})
ρ_w	Density of the water (kg/m^3)
ρ_o	Density of oil (kg/m^3)
ρ_m	Density of mineral fines (kg/m^3)
ρ_{OMA}	Density of a single OMA droplet (kg/m^3)

ρ_{OMAs}	Density of the OMAs (kg/m^3)
σ	Oil-water interfacial tension coefficient (N m^{-1})
$\hat{N}_{(r)}$	Number of droplets (per unit water volume)
V	Volume of oil within a unit volume of the mixing layer (m^3)
M_{OMA}	Mass of a single OMA droplet (kg)
M_o	Mass of the oil droplet within the OMA droplet (kg)
M_m	Mass of the mineral fine within the OMA droplet (kg)
d_o	Diameter of oil droplet (m)
d_m	Diameter of mineral fines (m)
d_{OMA}	Diameter of a single OMA droplet (m)
d_{max}	Maximum oil droplet diameter (m)
$d_{OMA\,i}$	Diameter of the i-th OMA droplet contained in OMAs droplets (m)
D_{OMAs}	Average diameter of OMAs (m)
D_{fc}	Characteristic size of OMAs (m)
N	Number of mineral fines covering on the oil droplet
F	3D fractal dimension of OMAs droplets ($F<3$)
Φ	Effect of the size distribution
α	Shape-related coefficient
β	Shape-related coefficient
Λ	Mixing factor
K	Oil mass exchange rate coefficient

M_a	Total mass of the spilled oil (kg)
M_s	Mass of oil in the slick (kg m^{-2})
M_e	Mass of oil in the mixing layer, respectively (kg m^{-2})
λ_{wo}	Resurface rate (s^{-1})
λ_{ow}	Entrainment rate (s^{-1})
L_{wo}	Vertical length-scale parameter (m)
L_{ow}	Vertical length scale parameter (m)
$\mathrm{w}(\mathrm{r}_\mathrm{l})$	Mean terminal velocity of the rising droplets (m/s)
k_b	Coefficient of the dissipated wave energy (0.3–0.5)
γ	Dimensionless damping coefficient
D	Vertical diffusion coefficient (m^2/s)
L_d	Vertical length-scale (m)
b	Oil evaporation rate (s^{-1})

List of Acronyms

ANS	Alaska North Slope Crude Oil
CFD	Computational Fluid Dynamic
GSD	Geometric Standard Deviation
GUI	Graphical User Interface
LISST	Laser In Situ Scattering and Transmissometer
LNS	Layer Averaged Navier-Stokes
MESA	Medium South American crude oil
U.S. MMS	U.S. Minerals Management Service
MOSM	The Multiphase Oil Spill Model
OCS	Outer Continental Shelf oils
OHMSETT	Oil and Hazardous Simulated Environmental Test Tank
OMAs	Oil-Mineral Aggregates
OMA-SIM	Oil Droplet and OMAs Simulation
PB	Plunging Breaking wave
PSU	Practical Salinity Units
RNB	Regular Non-Breaking wave
SB	Spilling Breaking wave
WTI	West Texas Intermediate oil

Chapter 1

Introduction

1.1 Background

Oil spills can result in significant contamination of ocean and shoreline and have adverse effects on both human and aquatic lives. Oil spills accident events have been reported widely, for instance, the Exxon Valdez accidental spill results in 35,500 tonnes of crude oil dispersed into the ocean near Alaska in 1989 (Page et al., 2005). The effects of this contamination lasted 20 years and it disturbed and even ruined the normal life of local residents. These accidental oil spills stimulate in studies of oil spill mechanism, remediation instruments, and in prediction models.

Crude oil is mainly dispersed in the form of micron-sized droplets. In nearshore waters, oil droplets may aggregate with natural mineral fines. These mineral fines and oil droplets may aggregate together and form agglomerates commonly referred to as Oil-Mineral Aggregates (OMAs) (Lee et al., 2008), which is a natural process that enhances dispersion of spilled oil in aquatic environments. The formation of OMAs is affected by properties of oil and mineral fine, and by the environmental condition.

A number of investigations have been carried out on OMAs in the near shore region in order better understand oil dispersion. Bragg et al. (1994) found that OMAs formation enhanced the natural cleaning and removal of stranded oil by making oil less adhesive and easier for hydrocarbon-degrading bacteria to break down. Lee et al. (1997) found that OMAs enhanced the biodegradation of crude oils. Whitby et al. (2008) reported that mineral fines played a surfactant role to prevent suspended oil droplets from coalescing and reforming an oil slick. The results of shoreline field trials (Lee et al., 1997, 1998; Lunel et al., 1997; Owens and Lee, 2003; Li et al., 2009) and laboratory experiments (Cloutier et al., 2002; Omotoso et al., 2002; Stoffyn-Egli and Lee, 2002) indicated that the formation of OMAs in the near shore environment enhanced the natural dispersion of oil spills.

Mineral fines covering the surface of oil droplets to form OMAs are thought to be capable of stabilizing oil droplets. The stabilization of individual oil droplets coated by suspended mineral fines in water, has been reported in some literatures (Bragg and Yang, 1995; Lee et al., 1996, 2003; Muschenheim and Lee, 2002). The effectiveness of the mineral fines in stabilizing oil droplets in water depends on several factors, such as the size and wettability of the mineral fines. Mineral fines stabilize oil droplets by attaching to the oil-water interface where they form rigid films to prevent the coalescence of oil droplets. Electrically charged mineral fines at the oil-water interface also enhance the stability of oil droplets. The size of mineral fines selected as oil droplets stabilizers is an important factor. Bragg and Yang (1995) designate a diameter (< 4 μm) as for the size of the mineral fines used to stabilize oil droplets. The wettability is another factor that affects oil droplets stabilization. Wettability is the degree to which a solid particle is wetted by oil or water when both are present. When the contact angle between solid particle and oil-water interface is less than 90°, the solid is preferentially water-wet. Similarly, when the contact angle is greater than 90°, the solid is preferentially oil-wet. Contact angles close to 90° result in an intermediately wetted solid that generally leads to the stablest suspension. If the mineral fines remains entirely in the oil or water phase, it will not be an oil droplets stabilizer. For the mineral fines to act as an oil droplets stabilizer, it must be present at the oil-water interface and must be wetted by both the oil and water phases. In general, oil-wet mineral fines preferentially partition into the oil phase. Water-wet mineral fines preferentially partition into the water phase and prevent the coalescence of oil droplets.

Mineral fines, such as those composed of clay, can stick together in aquatic environments, into a higher order structure termed "floc". Oil droplets suspended in seawater and coated with mineral fines can also flocculate in seawater. Multiple oil droplets coated by mineral fines can stick together in higher order three-dimensional structure, forming natural Oil-Mineral Aggregates, which can have similar properties as clay flocs. Particularly, two phenomena occur during the formation of the OMAs. One is interaction between clays. Another is interaction between clays and oil droplets. A number of publications have described the interaction between clays. Jackson (1998) proposed that all suspensions of mineral fines were to some degree subject to flocculation. Here, flocculation was defined as the formation of larger particles of a solid phase dispersed in a solution by the gathering together of smaller particles. Interaction behavior of clays is a function of the balance between repulsive electrostatic fields of the negatively charged clay particles and the attractive Van der Waals forces between them (Bassin and Ichiye, 1977). Clay particles normally have a negative charge due to the anions in the broken chemical bonds in the crystal lattice (Edelvang and Larsen, 1995). In a stable clay solution, the repulsive force predominates. If a small amount of electrolyte is added to the solution, the negative charge attracts positive cation which form a thin film around the particle to produce an electrical double-layer. This double-layer reduces repulsion and allows particles to form clay-oil floc emulsions.

Bragg and Yang (1995) suggest that clay-oil floc form due to the attraction between the eletrostatic charges on the surfaces of mineral fines, polar hydrocarbon molecules in the oil, and ions in the seawater. Polar charges in the oil result from heteroatoms such as nitrogen, sulfur, and oxygen. These are attracted to the positive charges on cations in seawater. A “cation bridge” is thus formed in the film of seawater between the mineral fines and the oil. Laboratory studies conducted by Bragg and Yang (1995) indicate that polar hydrocarbons are required for interaction to occur. A non-polar oil, consisting of the recombined saturate and aromatic fractions of weathered Exxon Valdez oil, did not flocculate with suspended fines following vigorous agitation. The polar fraction of oil plays an important role in the clay-oil interaction process. Interaction among the mineral fines themselves and the oil droplets occurs because mineral fines can generate varied surface charges due to uptake of H^+ and OH^- by oxides on minerals and by isomorphic substitution, rendering surfaces negative while carrying a positive charge on their edges (Ives, 1978). These types of interactions form OMAs, in which small oil droplets are coated with micron-sized mineral fines and are surrounded by seawater.

The reported OMAs size varied from system to system, depending on the type of oil, loading and type of suspended particles, and the mixing energy of the system (Lee, 2002; Khelifa et al., 2002; Guyomarch et al., 2002; Sterling et al., 2004; Li et al., 2007; Lee et al., 2008). Guyomarch et al. (2002) reported that the average size of the OMAs in the settled phase in a flask experiment varied from 50 to 1000 μm. Sterling et al. (2004) reported that the diameters of the suspended OMAs were between 10 and 100 μm at a sediment-to-oil ratio of 1:3. In a wave tank experiment, Li et al. (2007) observed that the diameter of OMAs was nearly 50 μm in the absence of chemical dispersants and 10 μm in the presence of dispersants.

Numerous studies have advanced our understanding of the mechanism of formation of OMAs (Lee and Stoffyn-Egli, 2001; Lee et al., 2008). The characteristics of OMAs and the factors affecting OMAs formation have been studied recently (Binks and Lumsdon, 2000; Lee et al., 2008). Formations of the OMAs were classified into three types by Stoffyn-Egli and Lee (2002), namely droplet, solid, and flake aggregates. Mineral fines mainly composed of kaolinite and quartz formed droplet aggregates whereas sediment dominated by montmorillonite formed flaky OMAs. The type of OMAs formed is controlled by the properties of the crude oil and mineral fines and by the environmental conditions, such as the type of waves.

The various factors affecting the formation OMAs include: 1) the physical properties of the oil such as composition, density, viscosity; 2) the physical properties of the mineral fines such as wettability, size and concentration; and 3) the physical properties of the dispersant; and 4) the environmental conditions such as wave energy dissipation rate, water temperature, pH, and salinity.

Wood et al. (1997) stated that the correlation is weak between mineral fines composition and the amount of oil trapped by OMAs. Guyomarch et al. (1999) investigated the interaction of oil and mineral fines with chemically dispersed oil and engineered clay. They conclude that there is no difference in OMAs formation with different clay minerals. The oil viscosity influences the ability of the oil to form droplets for a given amount of energy (Bragg and Yang, 1995). Delvigne et al. (1988) observed the formation of larger oil droplets with increasing oil viscosity, which indicates that the viscosity of the oil influences the size of the oil droplets. Temperature affects the physical properties of the oil. Viscosity decreases with increasing temperature of oil, so higher temperatures can enhance OMAs formation (Delvigne, 1988; Bragg and Yang, 1995; Wood et al., 1998; Stoffyn-Egli and Lee, 2002; Lee et al., 2003). Interfacial tension plays an important role in the OMA formation or emulsion stability. Fraser and Wicks (1995) reported that the maximum stable droplet size of dispersed oil could be obtained from the Weber Number, which is the ratio of inertial force to the interfacial tension. Oil droplets are stable at low interfacial tensions.

The effects of salinity on dispersed oils and mineral fines have been studied by investigators (Bassin and Ichiye, 1977; Meyers and Quinn, 1973; Bragg and Yang, 1995). Edelvang and Larsen (1995) debated whether mineral fines interaction needed salinity. Results from Payne et al. (1989) indicated that salinity had a strong controlling influence on reaction rates for dispersed oil droplets and the sediment types considered. Very low rates of reaction were observed for OMAs formation in freshwater, while substantially higher rates were observed in both 1.4-1.5 % and 2.8-3.0 % salinities.

Over the past decades, many oil spill models have been developed. Simulations of the breakup of surface oil slicks into small oil droplets and their vertical dispersion by breaking waves have been reported in some studies (Spaulding et al., 1992). The effects of droplet buoyancy, settling, oil evaporation, and turbulent conditions on kinetic mechanisms were the main concern of these models. A classical investigation on the relationship between oil droplet dispersion and turbulent energy was performed by Hinze (1955), who proposed an equation to calculate the maximum radius of an oil droplet as a function of the energy dissipation rate of breaking waves, the oil-water interfacial tension. Mackay et al. (1980) developed a model that proposed that the dispersion rate was inversely proportional to the oil-water interfacial tension and oil viscosity. Modeling vertical dispersion of oil by breaking waves has been developed in some studies (Huang, 1983; Reed et al., 1999). Clay particles have the properties of forming flocs when they exist in the water column. Numerical models have been proposed to study clay interaction, especially the relationships between density and size of flocs (Tambo and Watanabe, 1979; McCave, 1984; Kranenburg, 1994; Lau and Krishnappan, 1997; and Winterwerp, 1998). Modeling of the possible interactions between mineral fines and oil droplets was described by Hill and Nowell (1995).

Although modeling oil vertical mixing has been proposed by previous studies, few studies were found that detailed the interactions between oil droplets and mineral fines. The present study developed a new modeling approach, Oil Droplets and OMAs Simulation (OMA-SIM), which integrates an oil vertical mixing model with an oil droplets - mineral fines interaction model to simulate OMAs formation and oil/OMAs vertical mixing under breaking wave conditions.

1.2 Objectives

The principal purpose of this study is to develop a model OMA-SIM for simulation of the formation and vertical dispersion of oil droplets and OMAs. The specific objective of the thesis study is to develop a user-friendly computation system (OMA-SIM) to support the application of environmental friendly dispersant mineral fines, which includes:

1. Simulation of the formation of oil droplets by considering the effects of various wave energy dissipation rates on an oil slick;

2. Modeling of the behavior of OMAs with a density-based method;

3. Calculation of the concentration and particle size of oil droplets and OMAs and to predict how they change with time;

4. Examination of the key factors that affect the formation of OMAs and oil/OMAs dispersion;

5. Validation of the model with data from several experimental investigations and field tests and

6. Application of the developed OMA-SIM to filed cases.

1.3 Organization of the Thesis

The outline of this thesis is as follows. The problem statement, the research objective and the research framework have been presented in this chapter, together with background information about the problem. In Chapter 2, the literature related to modeling of oil/OMA formation, mixing and dispersion is reviewed. Reported wave tank experiments on study oil spills are also briefly summarized in this chapter. Chapter 3 describes the modeling approach developed for vertical mixing. The beginning of this chapter provides preliminary insight by introducing conceptual physical model including oil slick breaking up model, mixing layer model, and the formation of OMAs model. The rest of it describes detailed calculation approaches for processes of emulsification, evaporation, and resurfacing of oil/OMAs droplets. Chapter 4 validates the developed modeling approach through three case studies including wave tank experiments carried out by Lee et al. (2008) at Bedford Institute of Oceanography. Chapter 5 introduces a user-friendly computer system to support the modeling method and presents the modeling application for case studies. Conclusions, contributions and future research recommendations are presented in Chapter 6.

Chapter 2

Literature Review

This chapter reviews the previous work on oil spill modeling, identifies limitations of previous models, and describes the need for the development of a new model to describe the process of oil/OMAs vertical mixing.

The frequency of accidental oil spills in ocean environments is increasing and has led to the development of models to simulate the transport and fate of oil slicks. Oil spill models have usually been governed by complex processes consisting of advection, turbulent diffusion, spreading, evaporation, dissolution, dispersion, mixing, emulsification and so on. Over the past decades, many of these models described multiple processes focused on specific research objectives (Stolzenbach et al., 1977; Lee et al., 1990) and can be divided into two main categories. One class of models uses Eulerian and Lagrangian approaches to solve the advection-diffusion equation, to simulate oil dynamics in water (Tkalich, 2006). A second class of models uses kinetic equations to simulate the vertical mixing of oil droplets by breaking waves.

2.1 Oil spill modeling through advection – diffusion equations

Fay (1969) used layer averaged Navier-Stokes (LNS) equations to calculate the slick area, which provided the first popular model where the slick area calculation was derived asymptotically. In Fay's model, however, the main parameters for oil and water were not included. Some alternative empirical models have been developed to correct this flaw. Researchers discovered that dispersion rates were proportional to wind speed, and inversely proportional to the oil/water interfacial tension and oil viscosity. Mackay et al. (1980) reported a slick model that incorporated additional parameters such as wave dispersion rates with wind speed, the oil/water interfacial tension coefficient, and oil viscosity into his model. Both Fay's and Mackay's models considered the temporal dynamics of the slick area and postulate the slick shape to be circular or elliptical.

Based on the observation that oil droplets sink and resurface due to shear within the upper water layer, Johansen (1982) and Elliott (1986) proposed the hypothesis that the oil slick elongated in water. Elliott (1986) used the random walk technique to demonstrate the phenomenon of oil droplet movement within water. His research, however, did not include the slick dynamics on the water surface. Johansen (1982) obtained similar results using the Eulerian approach. Nihoul (1983) simplified the linearized Navier-Stokes (LNS) equations for turbulent flow and obtained a single non-linear transport-and-spreading (TS) equation that contributed to oil slick modeling importantly. The equation for slick thickness was derived and predicted temporal-and-spatial dynamics of the slick. Their research dealt with the slick area temporal dynamics in contrast to previous approaches. However, the computational cost to use the TS equation was too high to be accepted by users for that time.

Computational Fluid Dynamic (CFD) methods were developed to the appropriate accuracy and efficiency within the past two decades. In CFD models, priority is given to the description of the processes and solution techniques that directly affect slick advection and spreading, vertical mixing of oil droplets by breaking waves, and advection-diffusion of oil phases in the water column. Leonard (1979) reported the one-dimensional third-order-accurate QUICKEST algorithm that gave a significant boost to the development of upwind numerical schemes. Later, Leonard et al. (1995) developed a full two-dimensional version (UTOPIA) that utilizes 12-node computational stencil and 8-node flux expressions. Tkalich and Chao (2002) took into account the slick and subsurface oil, with kinetic exchange used to describe the vertical mixing between oil slick and mixing layer in their models. The Multiphase Oil Spill Model (MOSM) developed by Tkalich et al. (2003) attempts to utilize the recent advances to account for the major phenomena of oil behaviour in an aquatic environment. MOSM computes simultaneously six state variables: thickness of slick on the water surface; concentration of dissolved, droplet and particulate oil phases in the water column; and concentration of dissolved and particulate oil phases in bottom sediments. In these publications, different aspects of the model were addressed, including general formulation, oil droplet vertical exchange kinetics, the utility of numerical methods, and the model verification. Tkalich (2006) showed that only application of third-order (or higher) numerical schemes for the advective term could reduce the approximation error below the magnitude of the spreading term. Due to this fact, conventional (during the 1980s) first- and second-order numerical methods for solution of the TS equation predicted much higher slick spreading rates than were expected from measurements.

Boufadel (2006) investigated the combined effects of wave kinematics, turbulent diffusion, and buoyancy on the transport of oil droplets at sea using random walk techniques. In this study, the Monte Carlo Method was used to solve the convection-diffusion equation that describes the transport of oil. Six hundred oil particles were placed at the water surface and tracked for 500 wave periods. The study found that plumes that have large terminal rise velocities move faster forward but spread less than those that have small terminal rise velocities.

2.2 Oil vertical mixing modeling

According to observation and laboratory measurement (Li and Garrett, 1998; Delvigne and Sweeney, 1988), a mixing layer exists under oil slick. One can assume uniform mixing of the droplets within this mixing layer.

Various simulations of the breakup of a surface oil slick into small oil droplets and their vertical dispersion by breaking waves have been reported (Spaulding, 1988). Droplet buoyancy, settling, oil evaporation, and turbulence condition effects were the main kinetics mechanisms dealt with in these models. Classical investigations on the relationship between oil droplet dispersion and turbulent energy were performed by Hinze (1955) who proposed an equation to calculate the maximum radius of the oil droplets, which was a function of the energy dissipation rate of breaking waves, the oil-water interfacial tension, and oil viscosity. Mackay et al. (1980) developed a model that proposed that the oil dispersion rate was inversely proportional to the oil-water interfacial surface tension and oil viscosity.

The phenomenon of oil droplet vertical mixing in the water column was studied primarily by empirical or semi-empirical means. Earliest models employed the tabulated dispersion rate depending on oil type, sea state time after the spill. Johansen (1982) suggested first-order kinetics for the oil vertical dispersion, where wind speed is used to scale the breaking wave energy. Based on extensive laboratory experiments, Delvigne and Sweeney (1988) derived a relatively simple oil droplet entrainment model, elements of which are used in the majority of commercial and research oil spill models. The data obtained in the experiments of Delvigne and co-workers were regarded as the most extensive, and their empirical model the most complete. The entrainment rate initially was found to be inversely proportional to the oil kinematic viscosity.

2.3 Modeling Study of Oil Droplet and Mineral Fines Interaction

OMAs are composed of oil droplets and mineral fines and behavior as "flocs" in water. Numerous models on studying oil droplet and mineral fines interaction as a function of droplet size, shape and density have been undertaken. Garf (1971) discovered the effects of particles size on the flow regime near the settling particles and the consequent alteration of the drag force. Early attempts (Hawley, 1982; Van Leussen, 1988) demonstrated that the assumption of size-invariant density to predict the moving velocity of natural flocs was inappropriate and should be modified using empirical factors. According to the study of these controlling parameters of the moving process, Azetsu-Scott and Johnson (1992) reported that the density of aggregated droplets is difficult to measure directly and considered as the one of the parameters that most in need of further research. Modeling of the OMAs moving process depends on the understanding of the variability of OMAs density determined by oil droplet size, mineral fines' concentration, and environmental conditions such as temperature and salinity (Ajijolaiya, 2004).

Various models have been proposed to calculate the density of aggregated mineral fines (Tambo andWatanabe, 1979; Hawley, 1982; McCave, 1984; Lau and Kranenburg, 1994; Krishnappan, 1997). Most of them are regression functions particularly covering a narrow range of size and formation of the aggregated mineral fines. Based on a comparison between observation data and the results obtained with these models, a conclusion was made that the various models were successful at predicting density only over limited size ranges. The corresponding comparison for moving velocity data reveals similarly limited ranges of agreement between models and observation data. Reasonable prediction obtained with the models when the aggregated mineral fines less than 1000 μm.

2.4 Reported Wave Tank Experiments

Test tanks offer the potential for testing the dispersion of oil spill on a scale that approaches or is the same as that in the field. This review is a survey of wave tanks available for research on oil spills in North America.

Test tanks are typically classified into several categories, based on their primary use. Studies about using wave tank to test effectiveness of dispersants have been reported (Page et al., 1999; Ross, 2001; SAIC, 2003). Some research on studying hydraulics associated with oil spills have been conducted by wave tank tests (Page et al., 1998; Lambert, 2001). The wave tanks world wildly used were summarized as follows:

The U.S. EPA/BIO Tank was constructed under a Joint Project Agreement between Fisheries and Oceans Canada and the US Environmental Protection Agency. It was built at the Bedford Institute of Oceanography (Dartmouth, Nova Scotia, Canada). This wave tank is specifically to study oil spill associated dispersants and mineral fines. The tank is 32 m long by 0.6 m wide and 2 m deep, with a typical water depth of 1.2 m (Lee et al., 2002). Water is pumped directly from the adjacent Bedford Basin, which is connected to the Atlantic Ocean by Halifax Harbour. The tank has had many test runs with real oil in presence of dispersant and mineral fines (Lee, 2002; Lee et al., 2008; Li et al., 2007, 2009) since it was established.

OHMSETT (Oil and Hazardous Simulated Environmental Test Tank) was a tow tank typically built to test booms and advancing skimmers (Mullin and Lane, 2000). It is an only towing tank used for oil spill tests. The tank is larger comparing with other tanks and typically contains about 9,600 m^3 of brackish water pumped from the nearby bay. It is 203 m long, 20 m wide, and 3.4 m high, with a typical water depth of 32.4 m. Several relevant studies have been carried out at OHMSETT, including several dispersant tests.

The Texas A&M tank is a facility built to study the near shore dispersion of oil spills (Reilly et al., 1994). The facility consists of nine tanks equipped with computer-controlled wave generators, each tank 33.5 m long by 2.1 m wide and 2.4 m deep, with a typical water depth of 2 m. The maximum wave height could reach 0.6 m during test.

The Esso Tank was built for test dispersant effectiveness located in Calgary. The tank is 55 m long, 31 m wide, and 3.3 m deep, with a typical water depth of 1.9 m. up to a shallow portion of 1.9 m (Brown et al., 1985). A computer-controlled wave generator could be programmed to produce either regular or irregular waves. The maximum wave height could reach 0.3 m.

The SL Ross tank with a paddle wave generation system was built in Ottawa, Ontario, Canada. The tank is 11 m long and 1.2 m wide (Belore, 1985). Belore (2002) applied the tank to test the effectiveness of the oil spill dispersant Corexit 9500 on Hibernia oils at various temperatures of 0°C to 1°C.

2.5 Summary

Most previous model studies mainly focused on the fate and transport of oil droplets, however, there is a need for coupled experimental and modeling studies to provide more fundamental details to support the application of mineral fines as part of effective oil spill countermeasures. Oil vertical mixing model in presence of mineral fines was not concerned by previous studies. The published mineral fines interaction models were focused on the simulation of density of oil-mineral flocs. However, there are no models studied the density when oil coated with mineral fines and form OMAs. The present study integrates theories of oil droplet formation and vertical dispersion with oil droplet and mineral fines interaction mechanisms, to develop a new modeling approach (OMA-SIM) for simulation of the formation and vertical dispersion of oil droplets/OMAs by breaking waves.

Chapter 3

Model Development

3.1 Definitions

(1) Mineral fines: For our modeling studies, mineral fines are considered to be clay-size mineral matters. Mineral fines can flocculate and form flocs with each other and with oil droplets in seawater (Lee, 2002).

(2) Oil droplets: For our modeling studies, oil droplets are considered as spherical droplets. The size of oil droplets is determined by wave energy (Tkalich and Chan, 2002).

(3) Oil-Mineral Aggregates (OMAs) is the term that we use in our modeling studies to describe aggregation among various amounts of individual OMA droplets (Lee et al., 2008). An ideal individual OMA droplet is formed when an individual oil droplet is coated by mineral fines stuck to its' surface. In nature, each OMA is unique and contains a number of mineral fines of different sizes and shapes, and a variable number of oil droplets of different sizes, and may also contain bacteria and other components. The shape of an individual OMA droplet is considered as spherical in our model.

3.2 Conceptual Physical Model

3.2.1 Oil Slick Break-up Model

Oil slick broken into oil droplets and dispersed into water under breaking waves comprise a series of batch processes. Shaw (2003) addressed these processes in Figure 3-1. Oil droplets detached from a slick when a breaking wave collapse on to it. Air bubbles are dispersed into the water column concurrently. Then two competed processes occur. One process is oil droplets dispersed into water due to energy provided by breaking wave and gravity. Another process is that oil droplets coalesce and resurface by buoyancy to reform into oil slick. Dispersed air bubbles rising up and passing through the slick may entrain water into the slick thus improving the evaporation and changing the properties of the slick. Whether the oil droplets remain dispersed or coalesced depending on the slick properties, the size of the droplets and the frequency and intensity of the breakage wave.

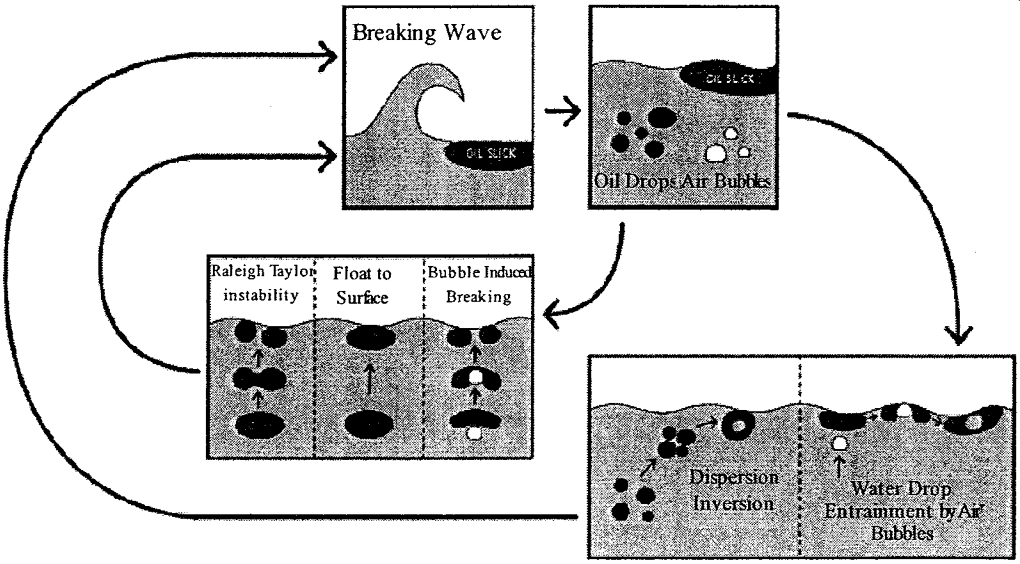

Figure 3-1 Oil dispersion under natural breaking wave conditions (Shaw, 2003)

3.2.2 Mixing Layer Model

Tkalich and Chan (2002) reported a mixing layer existed in the upper part of the water. Oil droplets are uniformly mixed due to breaking waves (Figure 3-2). In the mixing layer, the larger oil droplets may rise up and coalesce into the slick, whereas smaller droplets may dispersed downward into lower layers of the water. The oil mass exchange between the slick and the mixing layer is controlled by the oil droplet entrainment rate, the oil droplet resurfacing rate, and the fraction of large buoyant oil droplets. Below the mixing layer, vertical distribution of droplets is governed by advection and turbulent diffusion phenomena.

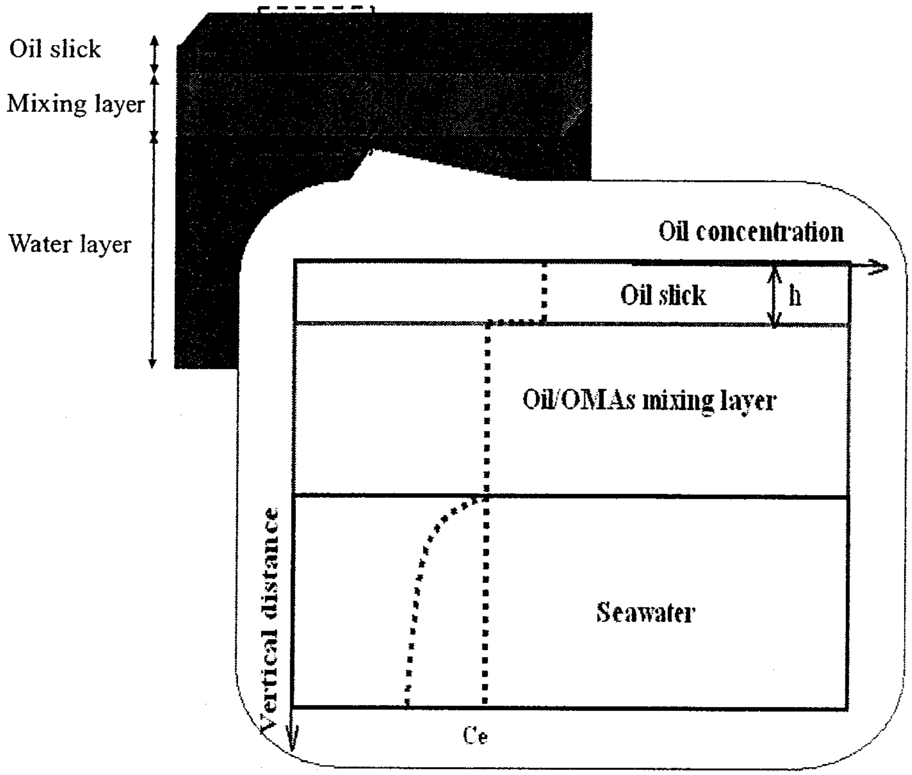

Figure 3-2 Sketch of the mixing layer

3.2.3 OMAs Formation Model

While in the presence of mineral fines, oil droplets (mentioned in 3.2.1 and 3.2.2) dispersed into water are covered by mineral fines. These oil droplets covered with mineral fines collide each other to form OMAs. This process is illustrated in Figure 3-3. The micro-sized mineral fines prevent oil droplets coalesce to form larger oil droplets. This reduces the probability of the large oil droplets to resurface and reform into oil slick for its high buoyancy. On the other hand, OMAs is preferentially dispersed into water because the density of OMAs is heavier compared with the density of oil droplets.

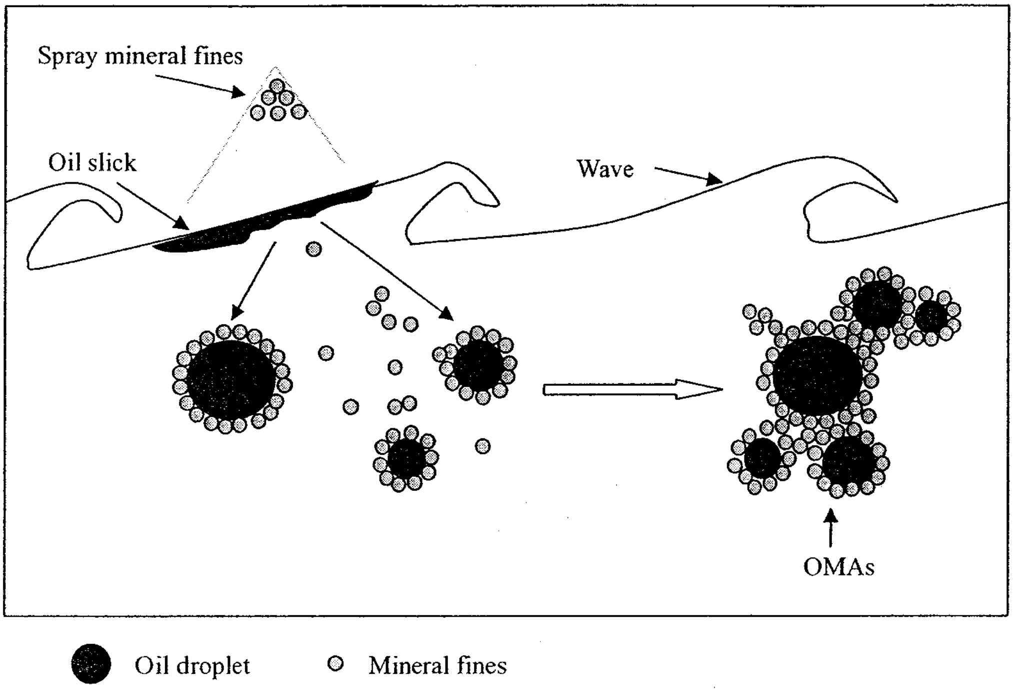

Figure 3-3 Sketch of the formation of OMAs

A variety of OMA structures have been formed in the laboratory tests (Lee and Stoffyn-Egli, 2001). IF30 oil and Bolivia sediment was used in the tests. The majority were individual OMA shown in Figure 3-4(a). Multiple droplet aggregates is illustrated in Figure 3-4(b).

3.3 Model design

The following study presents an approach that we have developed the OMA-SIM for modeling oil/OMAs vertical mixing in an oil spill event. A schematic description of the OMA-SIM is shown in Figure 3-5.

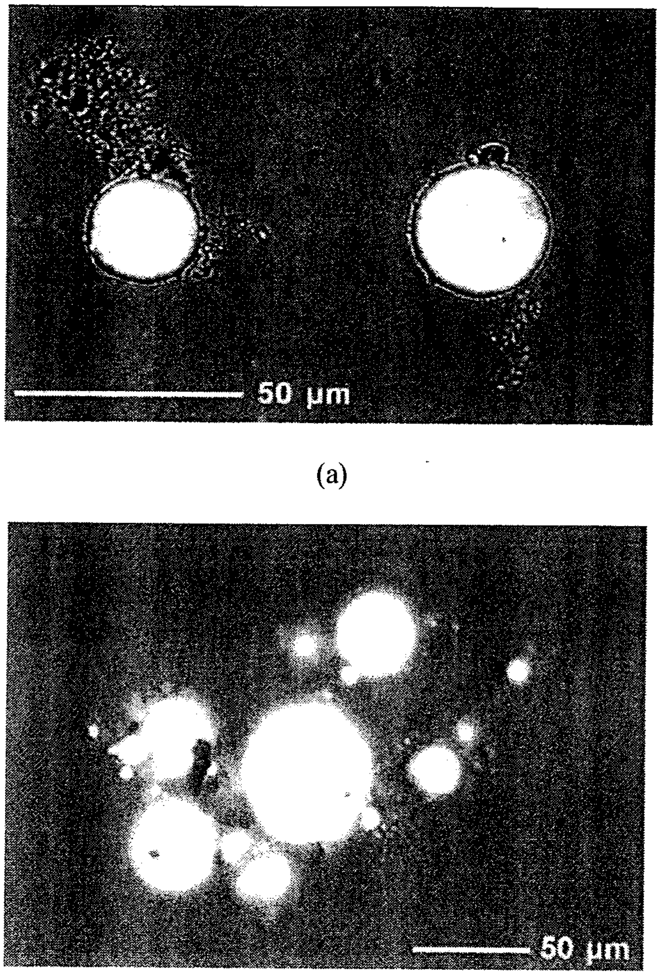

(a)

(b)

Figure 3-4 Observed OMAs in laboratory tests. (a) Individual droplet OMA, (b) multiple droplet OMAs (the oil droplets appear bright (fluorescent) and the mineral fines are darker) (Lee and Stoffyn-Egli, 2001)

3.3.1 Input Parameters

The input parameters of the OMA-SIM consist of 1) oil properties, 2) mineral fine properties, and 3) environmental (wave) conditions.

3.3.2 Framework of the Model

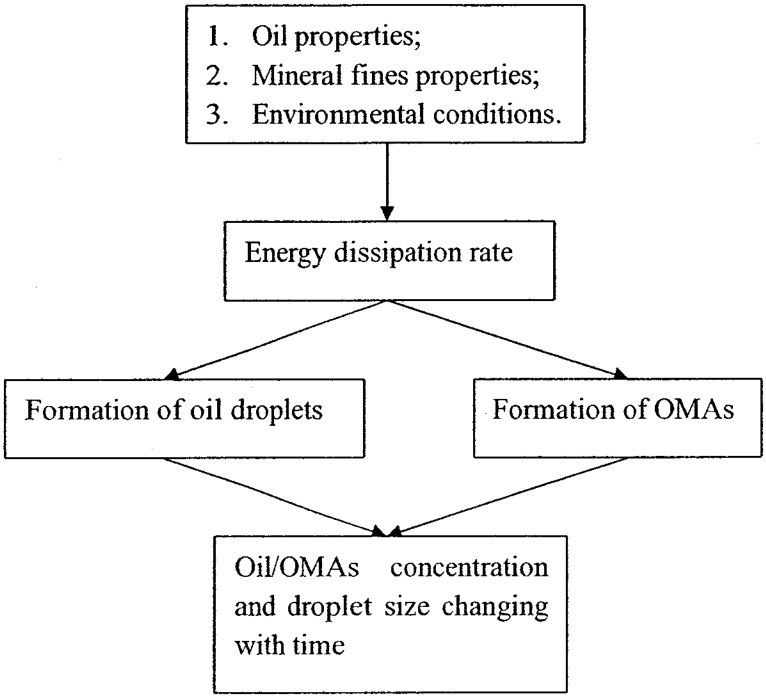

Figure 3-5 Schematic framework of the OMA-SIM

(1) The first stage of the OMA-SIM is to determine the effects of the different wave energy dissipation rates (ε), which are generated under different environmental conditions, on the maximum size of the oil droplet that can be formed. In this stage, the factors that affect oil droplets dispersion were concerned, such as oil density, viscosity, oil-water interfacial tension, water salinity/density, and temperature.

(2) The second stage of the OMA-SIM is to model the formation of OMAs, which result from the aggregation of oil droplets and mineral fines. The density of OMAs is calculated using the concept developed from oil droplet and mineral fines interaction

model. In this stage, density and size change resulted from generation of aggregates will affect the oil dispersion.

(3) The third stage of the OMA-SIM is then used to simulate oil/OMAs concentration and size as a function of time in wave tank

3.4 Technical Equations for OMA-SIM

3.4.1 Wave Energy Dissipation Rate

Breaking waves introduce significant amount of energy into the upper ocean layer. The resulted energy dissipation rate governs the formation and dispersion of oil droplet during an oil spill. The wave energy dissipation rate, ε, varies under different wave styles and environment conditions. During the past a few decades, many energy dissipation models have been proposed such as HK model (Hasselmann, 1974), BJ78 model (Battjes and Janssen, 1978), SN93 model (Southgate and Nairn, 1993), and RS98 model (Rattanapitikon and shibayama, 1998). Most of them were based on an empirical or semi-empirical formula calibrated from the experimental data. By comparing the accuracy of several existing dissipation models, we selected the RS98 model developed by Rattanapitikon and Shibayama (1998) to calculate the wave energy dissipation rate. The formula is below:

$$\varepsilon = KQ_b \frac{c_g g}{hH_b}\left[H_{rms}^2 - \left(h\exp(-0.58 - 2.00\frac{h}{\sqrt{LH_{rms}}}) \right)^2 \right] \tag{1}$$

where ε is the wave energy dissipation rate (m^2 s^{-3}), and K is the coefficient of the fraction waves with published value of 0.1, c_g is the wave group velocity (m s^{-1}), h is water depth (m), H_{rms} is the root mean square wave height(m), L is the wave length (m), Q_b is the fraction of the total number of waves that are breaking waves, which is derived based on the assumption that the probability density function of wave height can be modeled with a Rayleigh distribution truncated at the breaking wave height, H_b (m).

$$Q_b = -0.738\left(\frac{H_{rms}}{H_b}\right) - 0.280\left(\frac{H_{rms}}{H_b}\right)^2 + 1.785\left(\frac{H_{rms}}{H_b}\right)^3 + 0.235 \quad \text{for} \quad \frac{H_{rms}}{H_b} > 0.43$$

$$Q_b = 0 \quad \text{for} \quad \frac{H_{rms}}{H_b} \leq 0.43 \tag{2}$$

$$H_{rms} = \{\int_0^\infty h^2 dF(h)\}^{\frac{1}{2}} \tag{3}$$

$$F(h) = 1 - \exp(-\frac{1}{2}h^2/\hat{h}^2) \quad \text{for} \quad 0 \leq h < H_m\text{; and} \quad F(h) = 1 \quad \text{for} \quad H_m \leq h \tag{4}$$

where H_m is a maximum possible wave height for each depth h (m), $F(h)$ is the probability distribution of wave heights, the shape of $F(h)$ for the lower, non-broken wave heights is assumed to be same as it is in absence of wave breaking, i.e. of the Rayleigh-type, with modal value $\hat{h}$. Equation (4) represents a probability distribution with two parameters, $\hat{h}$ and H_m. All the statistics of the wave heights can therefore be expressed in terms of ($\hat{h}$, H_m).

A velocimeter is used to measure wave velocity, and then the wave period T can be calculated. The wave frequency can be evaluated by:

$$\omega = \frac{1}{\sqrt{2 \times \pi \times L / g}} \tag{5}$$

The wave length, L (m) and the wave period, T (s) have the relationship:

$$L = \frac{g}{2\pi} T^2 \tag{6}$$

so the wave velocity can be estimated from the above equation:

$$C = 2c_g = \frac{g}{2\pi} T \tag{7}$$

where C is the wave velocity (m s^{-1}).

3.4.2 Size of Oil Droplet

One of the key issues in oil spill modeling is the description of the phenomena of the formation of oil droplets, OMAs, and their size distribution and dynamics. Oil mixing near the surface can be affected by a variety of natural forces, of which the breaking wave phenomenon is the most powerful.

The maximum radius of an oil droplet was given by (Davis, 1985), and we used this formula also to calculate the maximum radius of an oil droplet containing in an OMA droplet:

$$r_{\max} = \frac{c_1}{2\rho^{0.6}\varepsilon^{0.4}}\left(\sigma + \frac{v_0\sqrt{2}(2\varepsilon r_{\max})^{1/3}}{4}\right)^{0.6} \tag{8}$$

here, c_1 is a constant from 0 to 0.363, r_{max} is the maximum oil droplet radius(m), v_o is the kinematic viscosity of the oil ($m^2\ s^{-1}$), ρ is the water density ($kg\ m^{-3}$), ε is the wave energy dissipation rate ($m^2\ s^{-3}$), and σ is the oil-water interfacial tension coefficient($N\ m^{-1}$).

3.4.3 Size Distributions of Oil Droplet

According to Delvigne and Sweeney (1988), the shape of steady-state oil droplet size spectra can be expressed as the power relationship $\hat{N}$ - r^{-s}. Based on the analysis of oil droplet sizes, the dimensionless droplet size is given by Tkalich and Chan (2002) below.

$$\hat{N}(r) = \frac{(3-s)V}{4\pi(r_{\max}^{3-s} - r_{\min}^{3-s})}\frac{1}{r^s}\ (s \neq 3) \tag{9}$$

where $\hat{N}$ is the number of droplets (per unit water volume), V is the volume of oil in all droplets within a unit volume of the mixing layer (m^3); and s is an empirical parameter, which is found to be 2.3 ± 0.06 in the experiment, though it may vary with the oil density and viscosity, weathering state, temperature, etc. $r_{\min}$ is minimum droplet radius (m).

Li et al. (2007) and Khelifa et al. (2002) further analyzed oil droplet size distributions, and how they were affected by oil composition (the ratio of asphaltenes and resins in the oil). The size distribution of oil droplets is described by the following equation:

$$N_t = \alpha(T) W_{ar}^{-0.64} \tag{10}$$

where N_t is the total number of droplets in 10^7/mL, W_{ar} is the ratio of asphaltenes and resins in the oil, and α is a function describing the effects of the temperature T. At temperature 0 and 20°C, α equals to 0.35 and 1.13, respectively.

3.4.4 Density-based OMAs Model

Here we assume that oil droplets, mineral fines are both spherical in shape. For a single OMA particle, the mass balance equation can be written as:

$$M_{OMA} = M_O + M_m \tag{11}$$

where M_{OMA} is the mass of a single OMA particle, M_o is the combined mass of the component oil particles within the OMA particle, and M_m is the combined mass of the mineral fine particles within the OMA particle, A hypothesis is proposed here that the size of mineral fines is far less than that of the oil droplets, and a single oil droplet with density of ρ_o (kg/m^3) and diameter of d_o (m) is coated entirely with N mineral fines with density of ρ_m (kg/m^3) and diameter of d_m (m). We can examine the density of a single OMA droplet as (Ajijolaiya, 2004):

$$\rho_{OMA} = \frac{\rho_o d_o^3 + N\rho_m d_m^3}{d_{OMA}^3} \tag{12}$$

where ρ_{OMA} is the density of a single OMA droplet. d_{OMA} is the diameter of a single OMA droplet. N is the number of mineral fines covering the oil droplet.

The diameter of a single OMA particle, d_{OMA}, is assumed to be approximately equal to the sum of the diameters of a oil droplet inside the OMA (d_o) and the sum of the diameters of all the component mineral fine particles surrounding the OMA (d_m), i.e., $d_{OMA} = d_o + d_m$.

N is the number of mineral fine particles covering the oil droplet: $N = \frac{4\pi(d_o + d_m)^2}{d_m^2}$

The mean oil droplet diameter can be written as (Spaulding et al., 1992):

$$\mathrm{d_o} = \frac{1}{2}\mathrm{d_{max}} \tag{13}$$

where the maximum oil droplet diameter, d_{max}, is given by (Davis, 1985):

$$d_{\max} = \frac{C_1}{\rho^{0.6}\varepsilon^{0.4}}\left(\sigma + \frac{\upsilon_O\sqrt{2}(2\varepsilon r_{\max})^{1/3}}{4}\right)^{0.6} \tag{14}$$

Based on the concept of fractal geometry, flocs of OMAs are formed when oil doplets collide with mineral fines in seawater. We assume that an idealized simple OMA is a single oil droplet that is covered by the mineral fines. When more than one OMA collide, they form multiple OMAs droplets with a larger size. The formation of OMAs droplets may appear as various shapes, sizes, and densities depending on the number of oil droplets and mineral fines contained in OMAs droplets.

The average density of OMAs droplets is calculated as:

$$\rho_{OMAs} = \rho_{OMA}\frac{\sum_{i=1}^{k} d_{OMA,i}^{3}}{D_{OMAs}^{3}} \tag{15}$$

where $d_{OMA\ i}$ represents the diameter of the i-th OMA droplet contained in OMAs droplets. D_{OMAs} is the average diameter of OMAs.

The average diameter of OMAs is expressed as (Jackson, 1998):

$$D_{OMAs} = \left(\sum_{i=1}^{k} d_{OMA,i}^{F}\right)^{1/F} \tag{16}$$

where D_{OMAs} is equal to diameter of the sum of the k OMA droplet and F is the 3D fractal dimension of OMAs droplets (F<3).

Combining Eq. (15) and Eq.(16) we obtain the boundary conditions of Eq. (15), where κ is the number of OMAs present in the floc:

$$\rho_{OMAs} = \rho_{OMA,} \quad \text{at } k = 1;$$

$$\rho_{OMAs} = \rho_w \quad \text{at } k = \infty.$$

Considering a simple linear variation of ρ_{OMAs}, we have:

$$\rho_{OMAs} = \rho_{OMA}\left[C_1 \frac{\sum_{i=1}^{k} d_{OMA,i}^3}{(\sum_{i=1}^{k} d_{OMA,i}^F)^{3/F})} + C_2 \right] \tag{17}$$

where C_1 and C_2 are constants could be calculated from the above conditions..

Eq. (17) can be solved considering the boundary conditions above, as:

$$\rho_{OMAs} - \rho_w = (\rho_{OMA} - \rho_w)\frac{\frac{\sum_{i=1}^{k} d_{OMS,i}^3}{k}}{(\frac{\sum_{i=1}^{k} d_{OMA,i}^F}{k})^{3/F}} \tag{18}$$

Eq. (18) becomes:

$$\rho_{OMAs} = \rho_w + (\rho_{OMA} - \rho_w)k^{(F-3)/F}\phi \tag{19}$$

with $m_3 = \frac{\sum_{i=1}^{k} d_{OMA,i}^3}{k}$, and $m_F = \frac{\sum_{i=1}^{k} d_{OMA,i}^F}{k}$

where ρ_{OMAs} is the density of the multiple OMAs, ρ_{OMA} is the density of an individual OMA droplet present in the flocs of OMAs, and ρ_w is the density of the water. The term $k^{(F-3)/F}$ represents the effects of the fractal dimension and of the flocs size, and Φ is the effect of the size distribution of the OMA particles forming the OMAs, so that:

$$\phi = \frac{m_3}{m_F^{3/F}} \tag{20}$$

F is the three-dimensional fractal dimension of the population of OMAs, and is given by:

$$F = \alpha \left(\frac{D_{OMAs}}{d_{OMA}} \right)^{\beta} \tag{21}$$

where α and β are shape-related coefficients and equal 1 for spherical particles (Winterwerp, 1998).

Using the boundary conditions,

$$F = \begin{cases} 3 & at \quad D_{OMAs} = d_{OMA} \\ F_c & at \quad D_{OMAs} = D_{fc} \end{cases} \tag{22}$$

the coefficient α and the exponent β are given by:

$$\alpha = 3 \text{ and } \beta = \frac{\log(F_c / 3)}{\log(D_{fc} / d_{OMA})} \qquad (23)$$

According to the fractal model of Meakin (1988), the equivalent spherical diameter of the population of OMAs is:

$$D_{OMAs} = d_{OMS} k^{1/F} \qquad (24)$$

Using Eq. (24) in Eq. (19), we have:

$$k^{(F-3)/F} = (k^{1/F})^{(F-3)} = \left(\frac{d_{OMA} k^{1/F}}{d_{OMA}} \right)^{F-3} = \left(\frac{D_{OMAs}}{d_{OMA}} \right)^{F-3} \qquad (25)$$

The model for the effective density of OMAs can be converted into the form:

$$\rho_{OMAs} = \rho_w + (\rho_{OMA} - \rho_w) \left(\frac{D_{OMAs}}{d_{OMA}} \right)^{F-3} \phi \qquad (26)$$

3.4.5 Oil Droplets and OMAs Vertical Dispersion

The effects of downward-directed mixing and the upward buoyant movement of spilled oil are combined to yield (Tkalich and Chan, 2002):

$$\frac{dM_e}{dt} = K(\Lambda M_s - M_e) \tag{27}$$

where Λ is the dimensionless "mixing factor", the most important characteristics of the oil, waves and water column are combined into a single "mixing factor". This mixing factor includes additionally the interfacial surface tension coefficient and oil density. K is the oil mass exchange rate coefficient. M_s and M_e are the mass of oil in the slick and the mixing layer, respectively (kg m^{-2}). To maintain a mass balance in the mixing layer, the oil mass in the slick has to follow the kinetics shown below:

$$\frac{dM_s}{dt} = -K(\Lambda M_s - M_e) \tag{28}$$

$$\Lambda = \frac{\lambda_{ow}}{\lambda_{wo} B_1} = \frac{k_b \gamma \omega H L_{wo}}{16 \alpha L_{ow} w(r_1) B_1} \tag{29}$$

$$K = \frac{(\lambda_{ow} + \lambda_{wo}) \lambda_{wo} B_1}{\lambda_{ow} + \lambda_{wo} B_1} \tag{30}$$

$$B_1 = \frac{r_{\max}^{3-s} - r_c^{3-s}}{r_{\max}^{3-s} - r_{\min}^{3-s}} \tag{31}$$

here, λ_{wo} is the resurface rate (s^{-1}), indicating the mass ratio of the large droplets moving from the mixing layer to the slick layer per unit time, which can be defined by:

$$\lambda_{wo} = w(r_1) / L_{wo} \tag{32}$$

where L_{wo} is the vertical length-scale parameter (m), which depends primarily on oil buoyancy, and the vertical components of current velocity and diffusion. The mean terminal velocity of the rising droplets is calculated using the relationship: $w(r_1) = 0.5k_{w}(r^{p}{}_{\max} + r^{p}{}_{c})$ (Spaulding et al. 1992), where r_c is the threshold radius. λ_{ow} is the entrainment rate (s^{-1}), indicating the exchange ratio of the oil droplet mass moving from the slick layer into the mixing layer per unit time, which can be defined by:

$$\lambda_{ow} = \frac{k_b \gamma \omega H}{16 \alpha L_{ow}} \tag{33}$$

k_b is the coefficient of the certain part of the dissipated wave energy expended to entrain the oil droplets from the slick into the water column. k_b may be evaluated from experiments and $k_b \approx 0.3\text{–}0.5$ (Lamarre and Melville, 1991); L_{ow} is the vertical length scale parameter (m); γ is the dimensionless damping coefficient; ω is the wave frequency; α is a dimensionless scaling factor that depends on the sea state (wave energy), $\alpha = 1.50 \pm 0.35$ (Delvigne and Sweeney, 1988).

The terminal velocity (m/s) is used as (Raj 1977):

$$w(r) = k_w r^p \tag{34}$$

where, p=2 and $k_w = 2g(1-\rho')/9\nu$ for Re < 50; p=0.5 and $k_{w'} = (16g(1-\rho')/3)^{1/2}$ otherwise; R_e=2rw/v is the droplet Reynolds number. This division of the rise velocity according the Reynolds number stems from an application of the Stokes law for small droplets and the Reynolds law for large ones.

Additionally, diffusion kinetics is considered in the vertical transport model:

$$\frac{dM_e}{dt} = -\frac{D}{L_d^2} M_e \tag{35}$$

where D is the vertical diffusion coefficient (m^2/s); L_d is the vertical length-scale (m).

Given that oil slicks are subject to rapid evaporation, a first order kinetics model is employed to account for evaporation losses:

$$\frac{dM_s}{dt} = -bM_s \tag{36}$$

where b is the oil evaporation rate (s^{-1}).

Combining the mixing, diffusion and evaporation processes, we obtain the integrated governing equations for droplet mixing kinetics at the oil slick-water column interface:

$$\frac{dM_s}{dt} = -K(\Lambda M_s - M_e) - bM_s \tag{37}$$

$$\frac{dM_e}{dt} = K(\Lambda M_s - M_e) - \frac{D}{L_d^2} M_e \tag{38}$$

where M_a is the total mass of the spilled oil in the slick and in the mixing layer (per unit area). Solving Equations (37) and (38), a set of deterministic models for computing changes of oil mass with time in the slick and mixing layers can be obtained.

3.5 Summary

A new mathematical modeling approach, which couples an oil vertical mixing model with an oil and mineral fines interaction model, has been developed to simulate the formation, vertical mixing of oil droplets and Oil-Mineral Aggregates (OMAs) in seawater. The key factors that affect vertical mixing, such as vertical diffusion, evaporation, and hydrodynamic dispersion, are integrated in this new modeling approach OMA-SIM.

Chapter 4

Model Validation

This thesis study describes a new modeling approach for oil spills that simulates changes in concentration and size of oil droplets and OMAs with time after the spill, as a function of breaking wave energy and the properties of oil, mineral fines, and dispersants. It includes five modules, as shown in Figure 4-1. Each module can be used to calculate the specific aspects of oil dispersion that are shown below:

Module 1: To calculate energy dissipation rate;

Module 2: To calculate maximum oil droplet diameter,

Module 3: To calculate density of OMAs;

Module 4: To calculate the entrainment rate, resurfacing rate, and mixing factor of oil droplets and OMAs;

Module 5: To simulate how the concentration and particle size of oil droplets and OMAs change with time after the spill.

4.1 Validation Case Study 1: The Effect of Wave Energy Dissipation Rate on Oil Dispersion – Numerically reproducing the BIO wave tank experiment from Lee et al. (2008)

The experiment described here was carried out in a wave tank at the Bedford Institute of Oceanography by Lee et al. (2008). Figure 4-2 shows a photograph of the wave tank facility together with a schematic diagram. The tank is 32 m long, 0.6 m wide and 2 m high. Waves were generated by a computer-controlled flap-type wave maker, which was situated at the left end of the tank. The average water depth was 1.50 m.

4.1.1 Materials and Wave Conditions (Lee et al., 2008)

Medium South American crude oil (MESA) was selected for the test. Two dispersants (Corexit 9500 and SPC 1000) and a without dispersant control (only oil) were tested in various combinations with MESA at three different wave conditions (regular non-breaking wave (RNB), spilling breaking wave (SB), and plunging breaking wave (PB)).

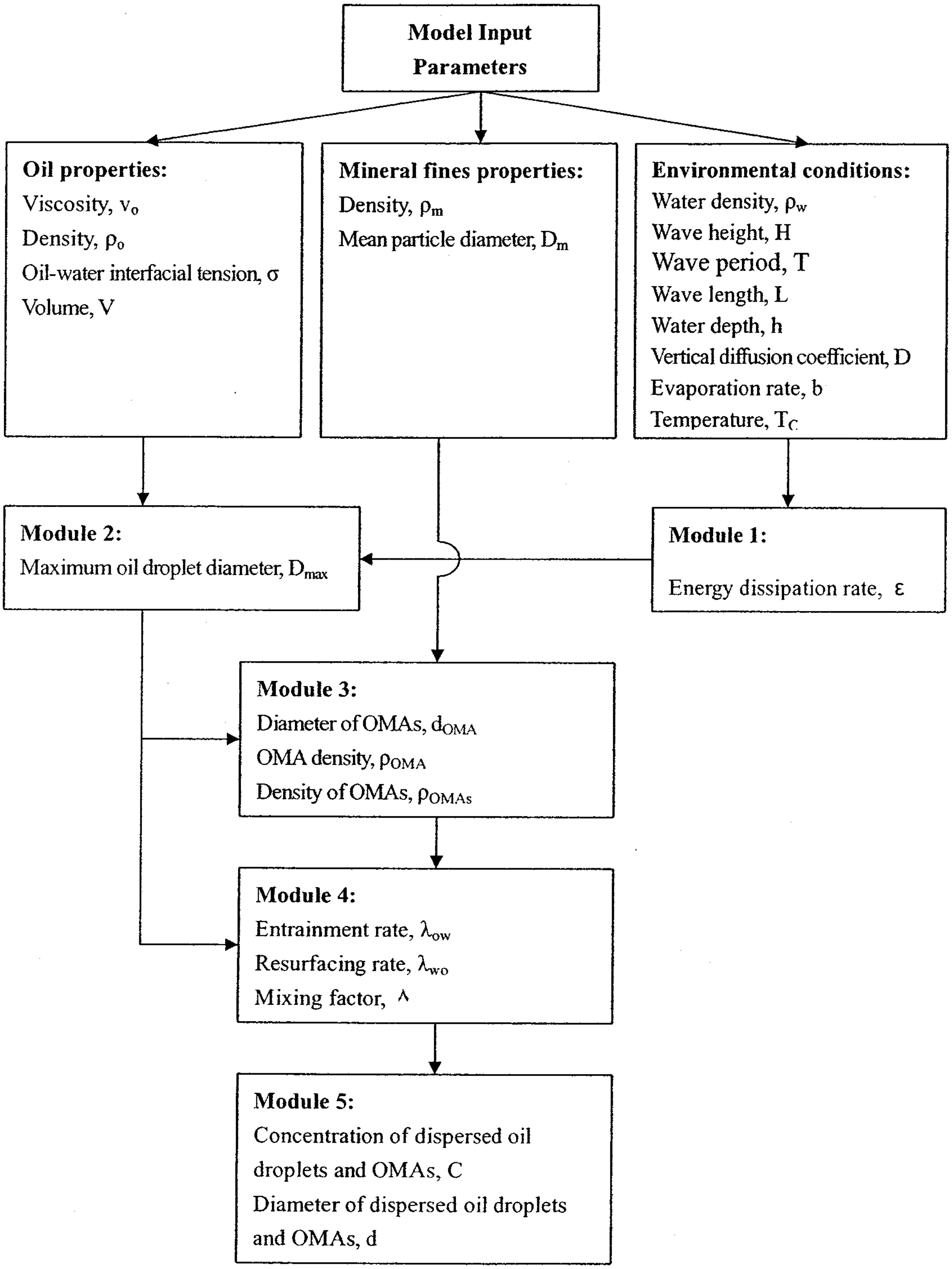

Figure 4-1 Flowchart of the OMA-SIM process

4.1.2 Oil Spill Wave Tank Experiment and Results (Lee et al., 2008)

300 mL of crude oil (MESA) were poured onto the surface of the water 10 m from the wave generation paddle to conduct the test. The dispersants were introduced by spraying on top of the oil immediately after oil addition. Samples were then collected and analyzed at three wave types with wave energy dissipation rates 0.005, 0.1, and 1 m^2/s^3, which represent regular non-breaking waves, spilling breaking waves, and plunging breaking waves, respectively.

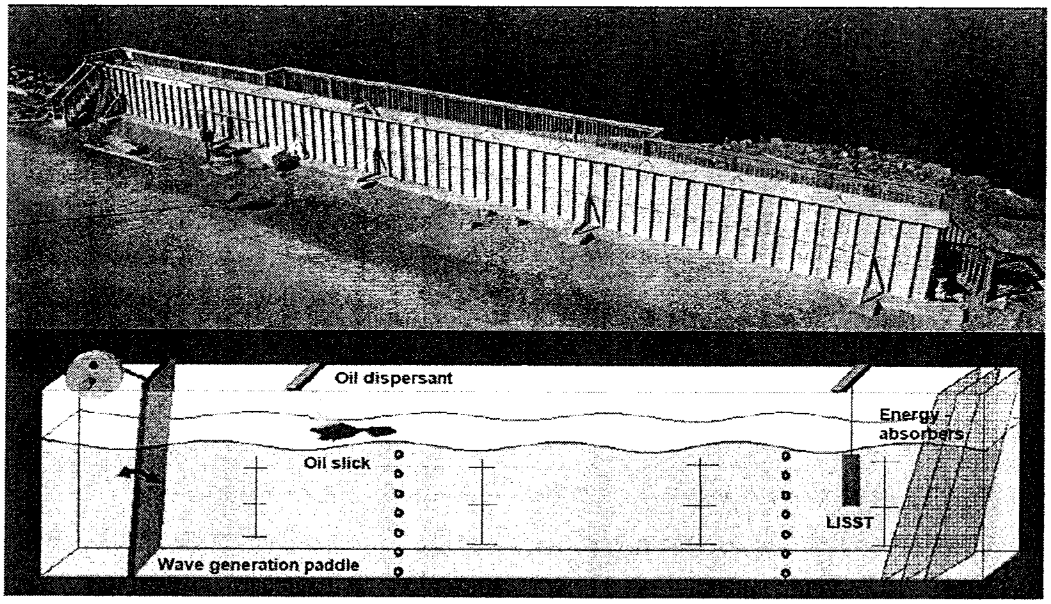

Figure 4-2 Wave tank facility at the Bedford Institute of Oceanography

(Lee et al., 2008)

The experimental results (Lee et al., 2008) for the effect of the wave energy dissipation rate on different combinations of MESA oil plus one dispersants (Corexit 9500 or SPC) and the control (only oil) are shown in Figure 4-3(a). These results are discussed in the next section (4.1.4) where the Lee et al. (2008) experimental results and the OMA-SIM results for validation case study 1 results are compared.

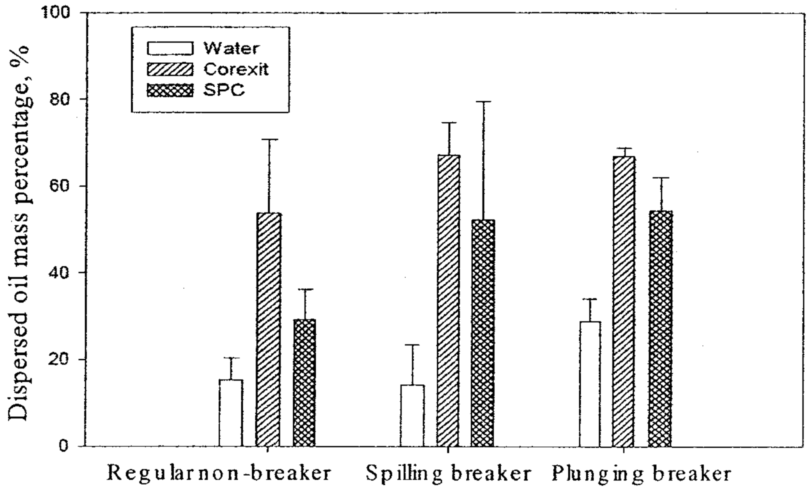

Figure 4-3(a) Experimental results of the effects of wave energy dissipation rate and dispersant on the dispersed oil mass (Lee et al., 2008)

4.1.3 Model Input – Case Study 1

The parameters shown in Table 4-1 (data from Lee et al., 2008) were used as input data for OMA-SIM, to simulate the experiment shown above in Figure 4-3(a). We named this our validation case study 1.

4.1.4 Modeling results – Case Study 1

The results from validation case study 1 are illustrated in Figure 4-3(b). A comparison of Figures 4-3(a) (Lee et al., 2008 experimental results) and 4-3(b) (OMA-SIM validation case study 1 results) indicates that in the absence of dispersant, the test oil was dispersed equally well by the two lower energy wave types (RNB and SB waves), and that the higher energy wave type (PB waves) was more effective in dispersing the oil by about 1.5-2 fold compared to the two lower energy wave types. The results indicate that wave energy is an important factor in oil dispersion. Higher wave energy dissipation rate induces more effective oil dispersion. The results also show that the presence of dispersants had a significant effect on oil dispersion at all wave energies tested and increased the dispersed oil mass percentage by about 2 to 3 fold compared to the control oil without dispersant. The results suggest that: 1) dispersants are effective in increasing oil dispersal by 2-3 fold, with the biggest effects seen at the lowest wave energies (RNB waves); and 2) Corexit 9500 and SPC 1000 are both effective oil dispersants, but Corexit 9500 is more effective than SPC 1000, again with the largest difference (about 2 fold) seen at the lowest wave energies.

Table 4-1: Input parameters for validation case study 1 (data from Lee et al., 2008).

OMA-SIM Input Parameters	Unit	Value
oil density (ρ_o)	kg/m^3	869
oil viscosity (υ_o)	m^2/s	69×10^{-6}
oil-water interfacial tension (σ)	N/m	0.002 - 0.0184
energy dissipation rate (ε)	m^2/s^3	0.005, 0.1, 1
the mass of spilled oil (Ma)	kg	0.13
water density (ρ_w)	kg/m^3	1027
water viscosity (υ)	m^2/s	10^{-6}
evaporation rate (b)	s^{-1}	2×10^{-5}
diffusion coefficient (D)	m^2/s	0.2

Comparing the validation case study 1 results (Fig. 4-3(b)) with the actual results of Lee et al. (2008) (Fig. 4-3(a)), we find that the model results are in agreement with the experimental results for MESA oil in the absence of dispersants.

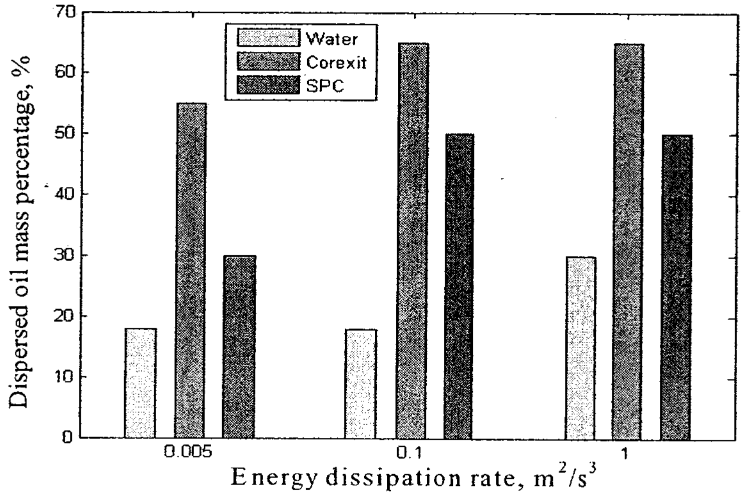

Figure 4-3(b) The OMA-SIM results of the effects of wave energy dissipation rate and dispersant on dispersed oil mass

4.2 Validation Case Study 2: The Effects of Chemical Dispersants and Mineral Fines on the Concentration and Size of Oil Droplet and OMAs - Numerically Reproducing the BIO Wave Tank Experiment from Li et al. (2007)

4.2.1 Materials and Wave Conditions (Li et al., 2007)

The test oil (MESA) and the dispersant Corexit 9500 were the same as used in validation case study 1. The effect of mineral fines (American Petroleum Institute kaolin) was tested in the presence or absence of the dispersant. The kaolin had a cation exchange capacity of 6.8 meq/100 g, a median particle size of 0.6 μm, and a density of 2.6 g/cm^3 (Li et al., 2007).

4.2.2 Oil Spill Wave Tank Experiment and Results (Li et al., 2007)

The wave tank was filled with filtered (5 μm) natural seawater from the Bedford Basin of Halifax harbor (with salinity of 30 practical salinity units (PSU)) (Li et al., 2007). MESA oil alone and in combination with Corexit 9500 dispersant or/and mineral fines were used for this experimental study. For the combination of oil and dispersant and mineral fines, before it was poured onto the surface of water, it was premixed in the flask at a mixing energy that reaches a level large enough to disrupt oil slick. The well mixed oil was then released onto the water surface of the tank. The samples were then collected and measured using Laser In Situ Scattering and Transmissometer (LISST) over a period of 0-200 minutes. It is assumed that the mineral fines coated the MESA oil droplets and formed OMAs. Figure 4-4(a) and Figure 4-5(a) illustrate how the concentration and the diameter of the oil droplets/OMAs changed with time after the experimental oil spill (Li et al., 2007).

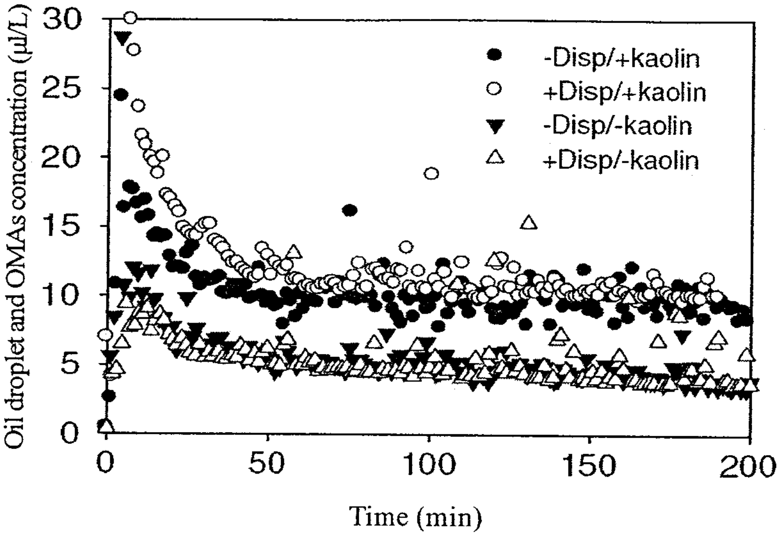

Figure 4-4(a) Experimental results of the effect of dispersant (Disp) and mineral fines (Kaolin) on oil droplets/OMAs concentration with time factor (Li et al., 2007)

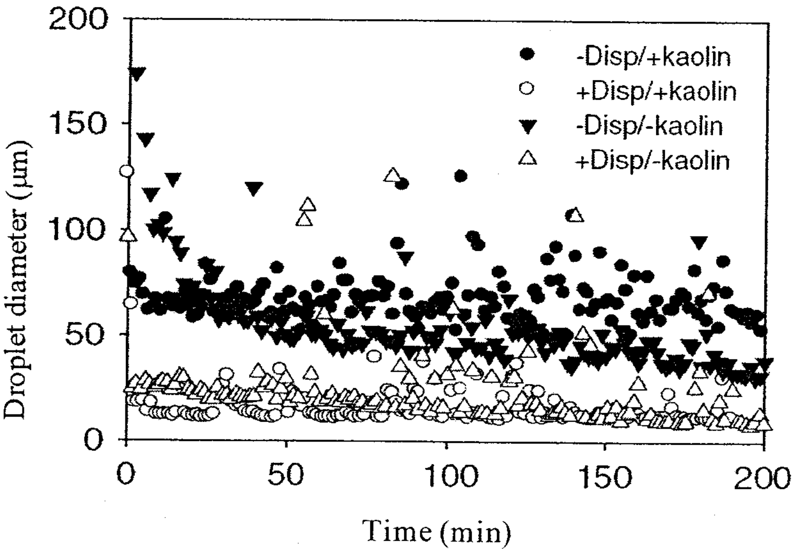

Figure 4-5(a) Experimental results of the effect of dispersant (Disp) and mineral fines (Kaolin) on oil droplets/OMAs diameter with time factor (Li et al., 2007)

(A) The Effect of Mineral Fines (Kaolin) Application on Concentration of Dispersed Oil/OMAs

The experimental results of Li et al. (2007) shown in Figure 4-4(a) indicate that the control oil (in the absence of mineral fines and dispersant; black triangles), the total dispersed oil droplet concentrations first increased to a maximum value of 10 μl/L within 10 minutes and then decreased gradually to a relatively constant value of 4 μl/L by 200 minutes. In the presence of mineral fines (black circles), however, the peak oil droplets/OMAs concentration was 3 fold higher (30 μl/L) at an early time (5 minutes), and then decreased gradually to a relatively constant value of 12 μl/L. The total droplet concentrations seen at the sampling device (LISST) in the presence of mineral fines were thus about 3 fold higher than in their absence, indicating that the mineral fines had a large effect on the oil dispersion in this experiment.

(B) The Effect of Dispersant (Corexit 9500) Application on Concentration of Dispersed Oil/OMAs

The dispersant Corexit 9500 did not appear to affect oil droplets/OMAs concentrations significantly in Figure 4-4 (a) (Li et al., 2007). If we compare the control (black triangles) with the plus dispersant (white triangles)), little difference is seen, probably due to the vigorous mixing caused by the breaking waves.

(C) The Effect of Mineral Fines (Kaolin) Application on Size of Dispersed Oil/OMAs

The experimental results (Figure 4-5(a) of Li et al., 2007) indicate that the initial diameter of the natural dispersed oil droplets was about 170 μm (black triangles) in the absence of either dispersant or mineral fines within the first few minutes of the experiment. After about 100 min, the control oil droplets gradually decreased in diameter to about 50 μm.

In the presence of the mineral fines (black circles) the diameter of the oil droplets immediately decreased the diameter of the oil droplets by about 2 fold to about 80 μm and they remained at this size (80 to 100 μm) until the end of the time period whereas the natural dispersed oil droplets became smaller (about 50 μm). Comparing with the natural dispersed oil droplets, the size of the oil droplets in presence of dispersant did not significantly changed.

(D) The Effect of Dispersant (Corexit 9500) Application on Size of Dispersed Oil/OMAs

As shown in Figure 4-5(a) from Li et al. (2007), the effect of dispersant (white triangles) was to dramatically affect and immediately reduce the droplet diameter 6 fold from the natural dispersed oil droplet (black triangles) of about 170 μm at time 0 minutes, to about 30 μm. At later times, the effect was still large and the dispersant reduced the natural dispersed oil droplet diameter from about 3 fold from 50 μm to about 15 μm at 200 minutes.

The experimental results of Li et al. (2007) shown above in Figures 4-4(a) and 4-5(a) are discussed below in comparison with the OMA-SIM results presented below in section 4.2.5.

4.2.3 Model Input – Case Study 2

Since the same oil (MESA) and detergent (Corexit 9500) was used as in validation case study 2, the input parameters for this case were as same as those presented in Table 4-1 (see Section 4.1.1). The additional data specific for validation case study 2 are provided in Table 4-2 below:

Table 4-2 Input parameters for validation case study 2 (data from Li et al., 2007)

OMA-SIM Input Parameters	Unit	Value
oil/water interfacial tension (σ)	N/m	0.0184
minimum oil droplet radius (r_{min})	m	10^{-6}
threshold oil droplet radius (r_c)	m	50×10^{-6}
mineral fines density (ρ_m)	kg/m^3	2600
mineral fines diameter (d)	m	6×10^{-7}
characteristic size of OMAs (D_{fc})	m	10^{-5}
three-dimensional fractal dimension of OMAs (Fc)	-	2
wave length (L)	m	1.56
wave height (H)	m	0.12

4.2.4 Modeling Results – Case Study 2

The results from validation case study 2 are illustrated in Figure 4-4(b) and Figure 4-5(b).

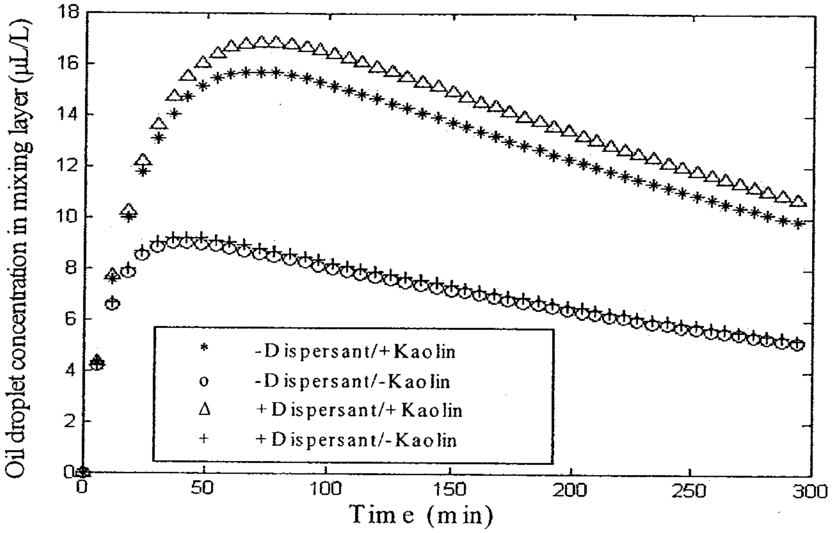

Figure 4-4(b) The OMA-SIM results of the effect of dispersant and mineral fines (Kaolin) on oil droplets/OMAs concentration with time

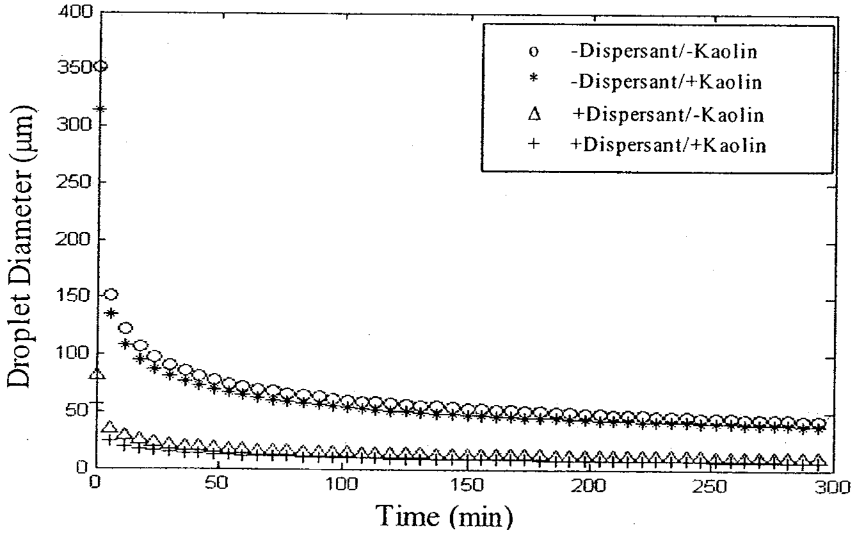

Figure 4-5(b) The OMA-SIM results examining the effect of dispersant and mineral fines (Kaolin) on oil droplets/OMAs diameter with time

4.2.5 Comparison of the Modeling Results and the Experimental Results from Li et al. (2007)

Comparison of the results of the validation case study 2 (Figure 4-4(b)) with the experimental results of Li et al. (2007) shown in Figure 4-4 (a), indicated that: 1) modeling results have the same trend with the experimental results; 2) in the presence of both chemical dispersant and mineral fines, the concentration of the oil/OMAs is always higher than in their absence; 3) the same large positive main effect of the mineral fines on oil dispersion but the magnitude was less (2 fold) compared to the experimental (3 fold); and, 4) a smaller effect of the dispersant on oil dispersion (0% to 10% in both validation case study 2 and the experiment of Li et al., 2007). Also, the time needed to reach the maximum value of oil concentration was later in the simulation (40 to 75 minutes) compared to the experimental value of 5 to 15 minutes). The reason for these discrepancies between experimental and modeling results may be due to: (1) the experimental conditions were not exactly the same as the nature ocean wave situations. The wind and current drive the waves in the natural environment, however, the effect of the wind was not taken account in the wave tank experiments; (2) some oil could be lost due to stuck onto the surface of the walls inside of the tank so that the concentration measured in experiment was lower than we the simulation results; (3) some mechanisms were not considered in the present model, such as chemical reaction between oil droplet and oxygen in seawater and biodegradation of dispersed oil. These mechanisms may reduce the level of oil droplets concentration;

(4) the samples of various combination of oil, dispersant, and/or mineral fines for each test was premixed vigorously before being introduced into the tank (Li et al., 2007), however, the mixing between oil, mineral fines, and dispersant would take a long period if it occurred in natural environment. Further studies (wave tank and field studies) would be required to know if early mixing effects are significant or not for the effective use of OMA-SIM for predicting oil dispersion in the presence of mineral fines and/or dispersant in a real oil spill situation.

The above experimental and simulation results shown in Figures 4-5(a) and 4-5(b) indicate that the dispersant Corexit 9500 has dramatically effects on reducing the size of dispersed oil droplets and OMAs. The presence of mineral fines did not reduce the diameters of the oil droplets comparing with the natural dispersed oil. However, the diameter of the oil droplets in experiment appears more scattered than OMA-SIM. A synergistic effect by chemical dispersants and mineral fines on the transfer of oil to dispersed phases is simulated in this study and this effect can be due to a number of contributing factors. First, dispersant reduce water-oil interfacial tension and stimulated the breakup of the oil slick (U.S. EPA, 2003). Second, mineral fines reduced the time period for the splitting of oil droplets into small and stable drops, which is otherwise a rate-limiting step for oil dispersion by microscale turbulence. Third, the interaction of mineral fines and oil reduced the buoyancy of oil droplets and therefore transferred more oil into the bulk aqueous phase (Lee, 2002; Owens and Lee, 2003). Mineral fines were reported to absorb oil at their surface due to their hydrophobic surface properties. Dispersants, while primarily reducing the oil/water interfacial tension, may also stimulate the interaction between oil and mineral fines. In summary, the results obtained from the validation case study 2 (Figure 4-4 (b) and 4-5(b)) were in agreement with the experimental results of Li et al. (2007; Figure 4-4(a) and 4-5(a)).

4.3 Validation Case Study 3: Numerically Reproducing the Prudhoe Bay Oil Experiment

Li and Garrell (1998) conducted an experiment investigating the breakdown of oil droplets under breaking waves generated in laboratory tanks containing an oscillating grid in a vertical tube 4 m high and 0.3 m wide. The size distribution of Prudhoe Bay Oil was measured at three different depths below the surface. Figure 4-6(a) gives examples of droplet size distribution measured in the experiments (Li and Garrett 1998).

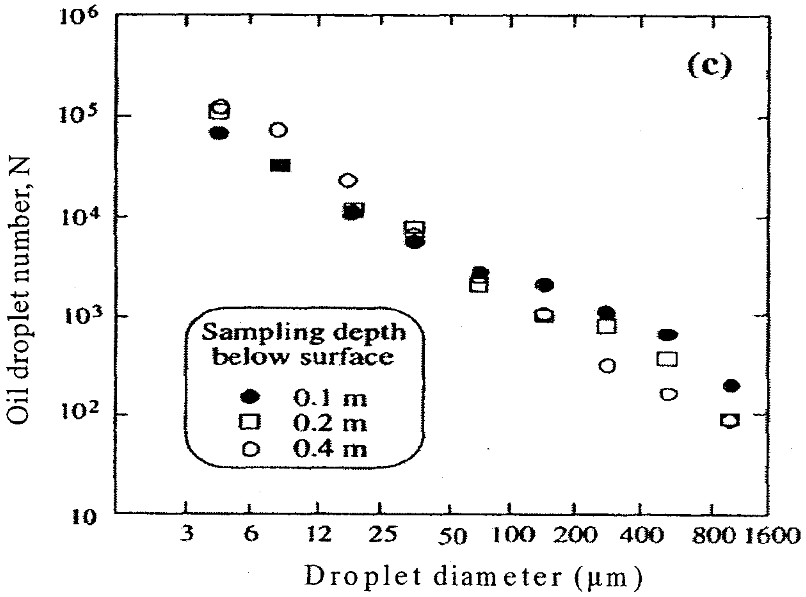

Figure 4-6(a) Experimental results for droplet size distribution measured in laboratory tanks (Li and Garrett, 1998)

4.3.1 Model Input – Case Study 3

Prudhoe Bay Oil has a dynamic viscosity of 0.1 kg $m^{-1}s^{-1}$, density of 900 kg m^{-3}, and oil-water interfacial tension of 10^{-2} N/m. The water density is taken to be 1000 kg m^{-3}. Wave energy dissipation rate is 474 m^2s^{-3} (Li and Garrett, 1998). Data from Li and Garrett (1998) was used for the input parameters.

4.3.2 Modeling Results – Case Study 3

We simulated the droplet size distribution of the Prudhoe Bay oil droplets based on the data from (Li and Garrett, 1998). Figure 4-6(b) shows the simulation results obtained using the OMA-SIM. The agreement between the experimental and the simulated results indicates that there is a log-log relationship between the number of oil droplets N and their size generated under breaking waves. The larger experimental droplets (> 150 μm) were fewer in number, while the smaller droplets (< 50 μm) were much more numerous. The model results are consistent with the experimental results and suggest that the assumption about the mixing layer is reasonable.

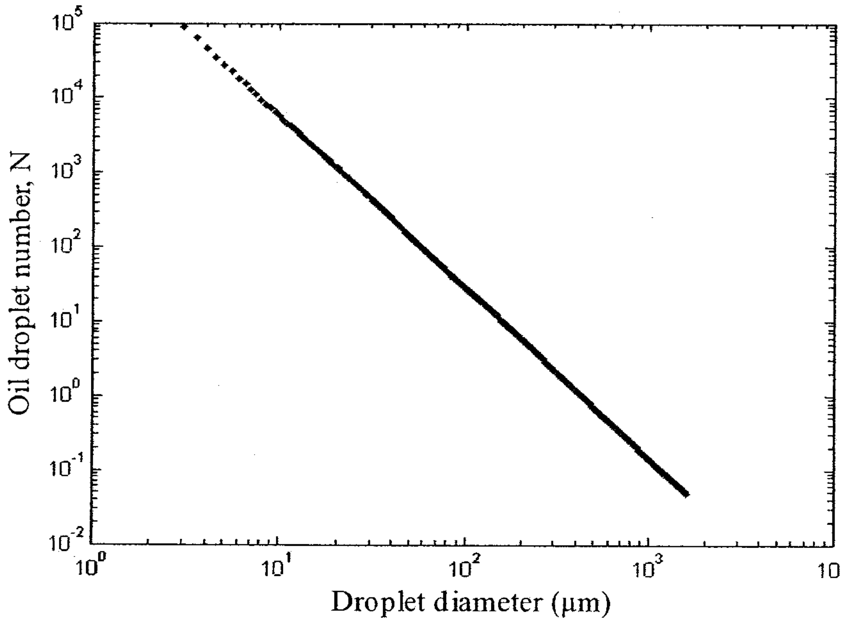

Figure 4-6(b) The OMA-SIM results of the droplet size distribution

Figure 4-7 shows the simulation of the cumulative mass frequency of oil droplets based on the data from (Li and Garrett, 1998). The size mass statistics of droplets showed that about 16% of the dispersed oil volume was presence as droplets less than 560 μm, more than 50% was presence as droplets larger than 1050 μm (diameter, or $d_{50\%}$), 84% of droplets were less than 1445 μm in diameter. The geometric standard deviation (GSD: $(d_{84\%}/d_{16\%})^{1/2}$), which reflects the variation of the droplet size, and is 1.61.

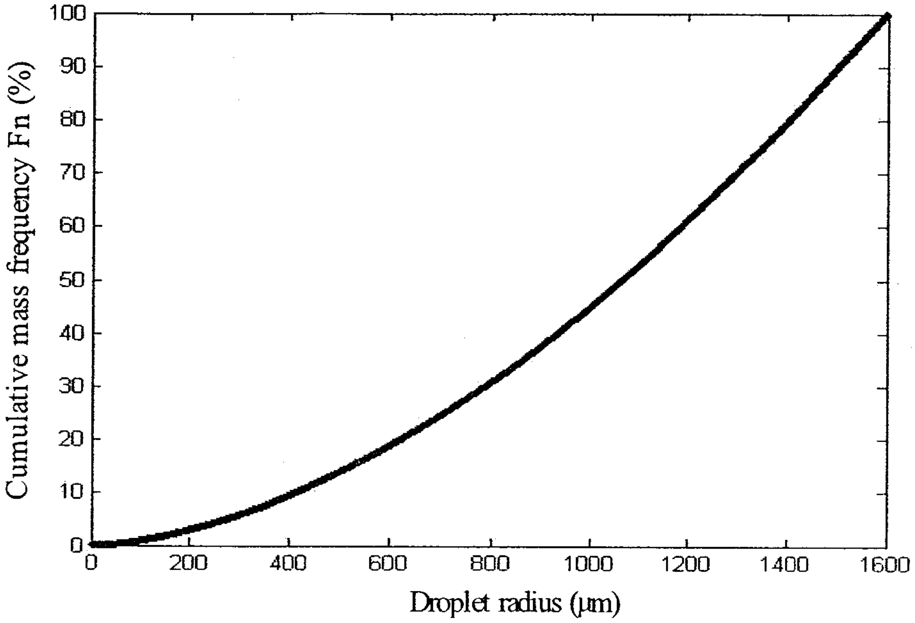

Figure 4-7 The OMA-SIM results of the cumulative mass frequency (%) vs. droplet radius (μm)

4.4 Summary of Validation Case Studies 1, 2, and 3

OMA-SIM developed in this study comprises five different modules which were used to examine wave energy dissipation rate, maximum diameter of oil droplets, average density of OMAs, and to simulate how the concentration and particle size of oil droplets and OMAs change with time.

The modeling results obtained from validation case study 1 are consistent with the experimental results and that wave energy dissipation rate and oil/water interfacial tension both play important roles in the simulation of oil dispersion after an oil spill. The value of oil concentration generated from the highest energy (plunging break wave condition; 1.0) is larger than that obtained from the other wave conditions. The addition of the dispersants significantly increased oil dispersion by reducing the oil/water interfacial tension and was most effective at the lower wave energy (regular non-breaking waves) and least effective at the highest wave energy (plunging breaking waves) (Figs. 4-3(a), (b)).

The validation case study 2 simulated the oil droplets and OMAs size distribution and concentration over time after an experimental oil spill (from 0 to 200 minutes). Comparison of the oil and OMA (oil + kaolin mineral fines) droplet sizes indicated that the mineral fines had a long term effects on droplet diameter; the presence of kaolin stablized smaller drop sizes at early times and increased the droplets size compared to natural dispersed oil at later times. The reason is that the aggregation between oil droplets and mineral fines caused the formation of flocs at later times (>100 minutes), which enlarged the droplets size and resulted in increasing the concentration of oil. The curves generated from validation case study 2 (Figure 4-4(b), 4-5(b)) have a similar trend compared with the experiment results (Figure 4-4(a), 4-5(a)), but there are some discrepancies between them. The discrepancy may result from factors , such as the concentration of mineral fines, shapes, salinity of the water, and so on. In a future study, the other factors will be introduced into the OMA-SIM.

Validation case study 3 illustrates the relationship between size of oil droplets and OMAs and their number in the mixing layer of the water during the oil vertical dispersion. Figure 4-6 shows the OMA-SIM results of the droplet size distribution of Prodhoe Bay oil, which is in agreement with the experiment results for mineral fines, dispersant and the synergistic combination of them together (Delvigne et al., 1988). The relation between cumulative mass frequency and droplet radius is illustrated in Figure 4-7, and the simulation results were similar to the experimental results reported by Li et al. (2007).

The OMA-SIM described here for simulating oil droplets and OMAs vertical mixing in seawater was developed in 5 modules and validated through the analysis of data from three case studies of published wave tank experiments. The results indicate that OMA-SIM can provide satisfactory vertical mixing simulation under wave tank environment conditions, and was most accurate for waves with high energies.

Chapter 5

Model Applications and Examination of Main Model Parameters through Four Case Analyses

The OMA-SIM developed for this thesis was programmed into a user-friendly system and is described in this chapter. A user's guide is provided to aid the user to operate the program and offers a step by step explanation on data input and program execution. A database containing the primary parameters for the properties of oil, dispersants and mineral fines, is provided to assist users to select reference data. Users can find parameters of interest, such as oil density, viscosity, and oil/water interfacial tension for some oils in the absence and presence of dispersant and/or mineral fines. The application of the program is illustrated in four case studies associated with field experiments.

5.1 Development of the OMA-SIM User-Friendly Interface System

5.1.1 Program Flowchart

Figure 5-1 illustrated the computation system flowchart for OMA-SIM.

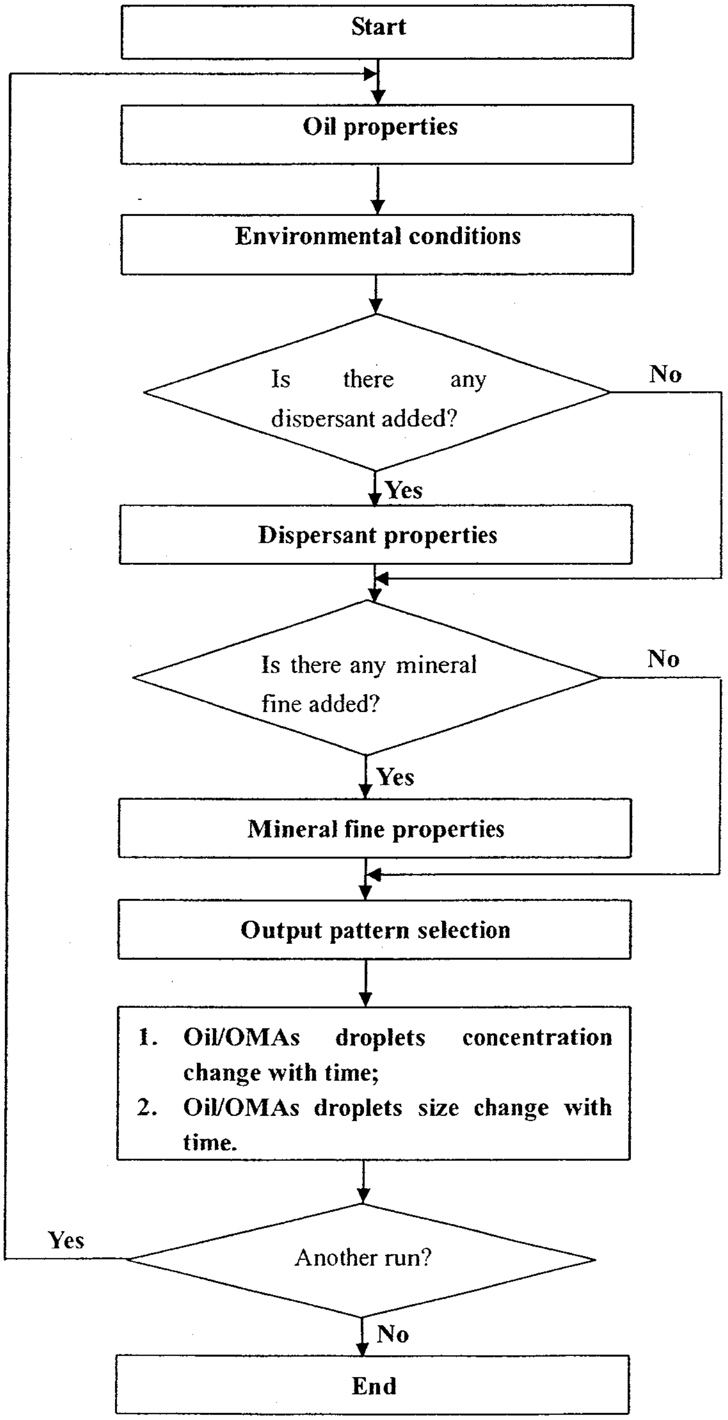

5.1.2 System Start up

The GUI (Graphical User Interface) program for OMA-SIM was developed using MATLAB® and m-file script. This interface was tested using the WindowsXP® platform. To use the OMA-SIM, the user must have MATLAB® because OMA-SIM is written with MATLAB® script language. To start the OMA-SIM, the user first defines the path using Path Browser in the MATLAB® command window. Alternatively, they can run the file OMASIM.m, stored under the path shown in Figure 5-2.

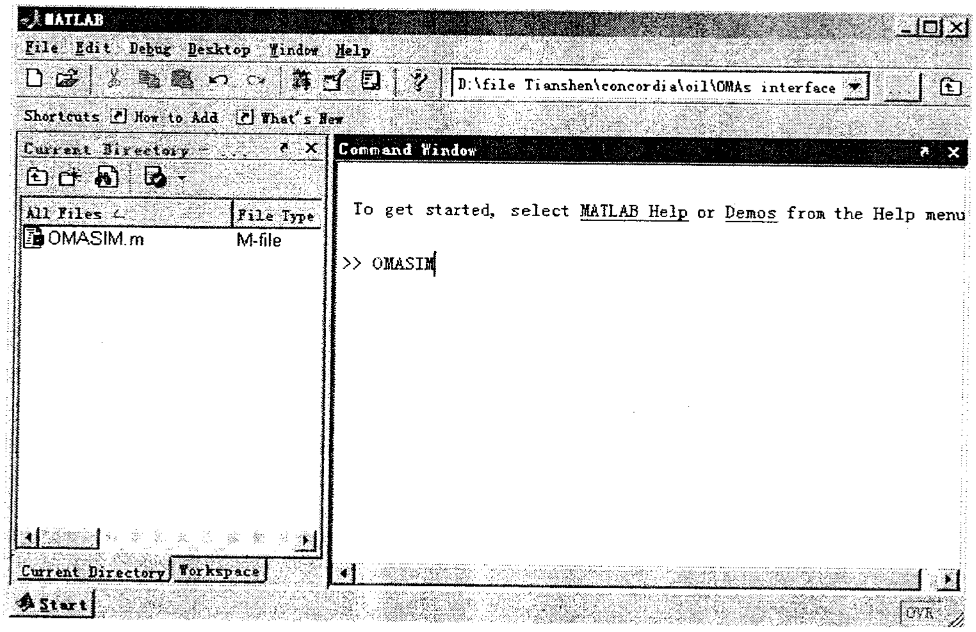

D:\file Tianshen\concordia\oil\OMAs interface

```
To get started, select MATLAB Help or Demos from the Help menu

>> OMASIM
```

Figure 5-2 The MATLAB® command window to define the path

5.1.3 The OMA-SIM Operation

In the user's training manual, we provide an example of a wave tank case study to help the user get familiar with this program. After the program starts, the model interface shows the message of the title and author message in Figure 5-3.

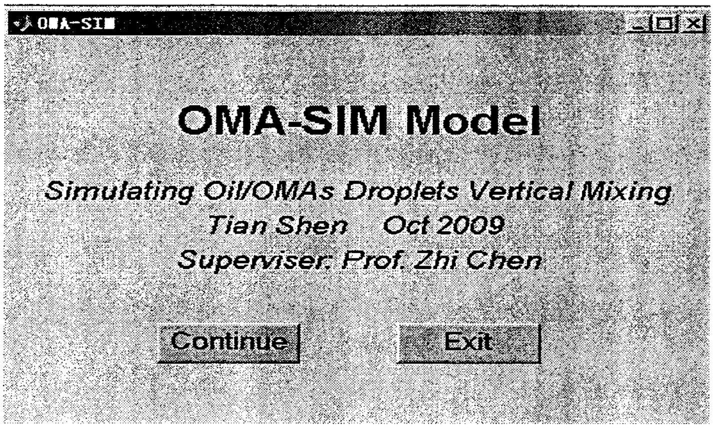

OMA-SIM Model

Simulating Oil/OMAs Droplets Vertical Mixing
Tian Shen Oct 2009
Superviser: Prof. Zhi Chen

Figure 5-3 OMA-SIM user interface

By clicking the 'Continue' button on the interface, user can proceed to the tasks selection.

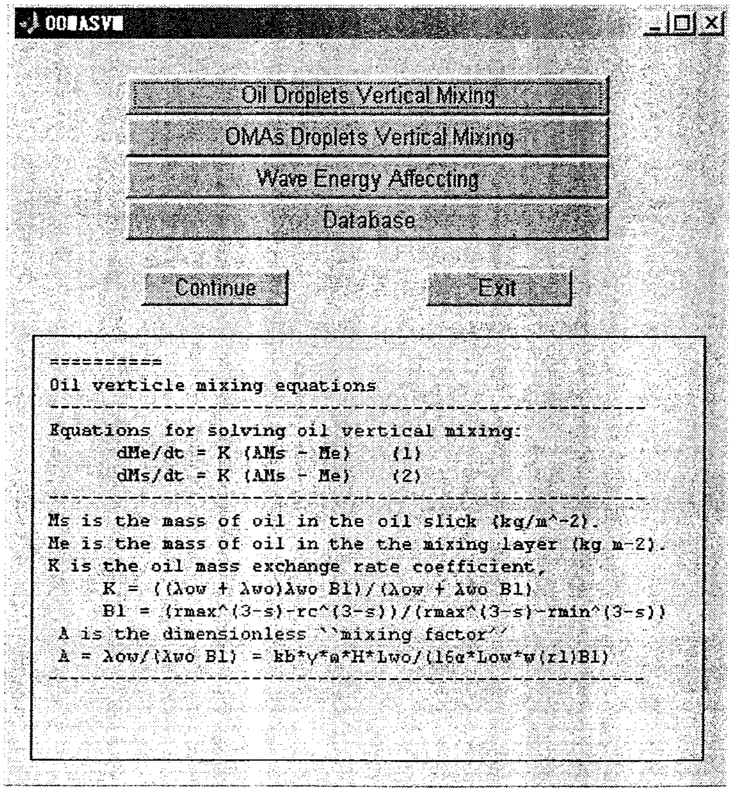

```
==========
Oil verticle mixing equations
-------------------------------------------------------
Equations for solving oil vertical mixing:
      dMe/dt = K (AMs - Me)    (1)
      dMs/dt = K (AMs - Me)    (2)
-------------------------------------------------------
Ms is the mass of oil in the oil slick (kg/m^-2).
Me is the mass of oil in the the mixing layer (kg m-2).
K is the oil mass exchange rate coefficient,
     K = ((λow + λwo)λwo B1)/(λow + λwo B1)
     B1 = (rmax^(3-s)-rc^(3-s))/(rmax^(3-s)-rmin^(3-s))
 A is the dimensionless ``mixing factor''
 A = λow/(λwo B1) = kb*γ*ω*H*Lwo/(16α*Low*w(rl)B1)
-------------------------------------------------------
```

Figure 5-4 Modules selection interface

The user can choose one of the three models to perform specific tasks, e.g. modeling oil vertical mixing, modeling OMA formation and vertical mixing, and study the effect of the wave energy dispersion rate on oil mixing. The user can obtain the references parameters by clicking the 'Database' button, which will link to an Excel file containing the reference parameters, to help the user to select or check their input parameters. After selecting one of top three modules, a text box containing a brief summary of the relative theory is loaded. After that, users are asked to input parameters used for the model. After inputting the proper value for the parameter, press the button 'Run' and the program will calculate the concentration and oil/OMA droplets size with time. When the calculation is complete, the figures showing droplet concentration and diameter are automatically generated and user can see the graphical results. Figure 5-5 illustrates the input parameters and OMA-SIM results for oil vertical mixing.

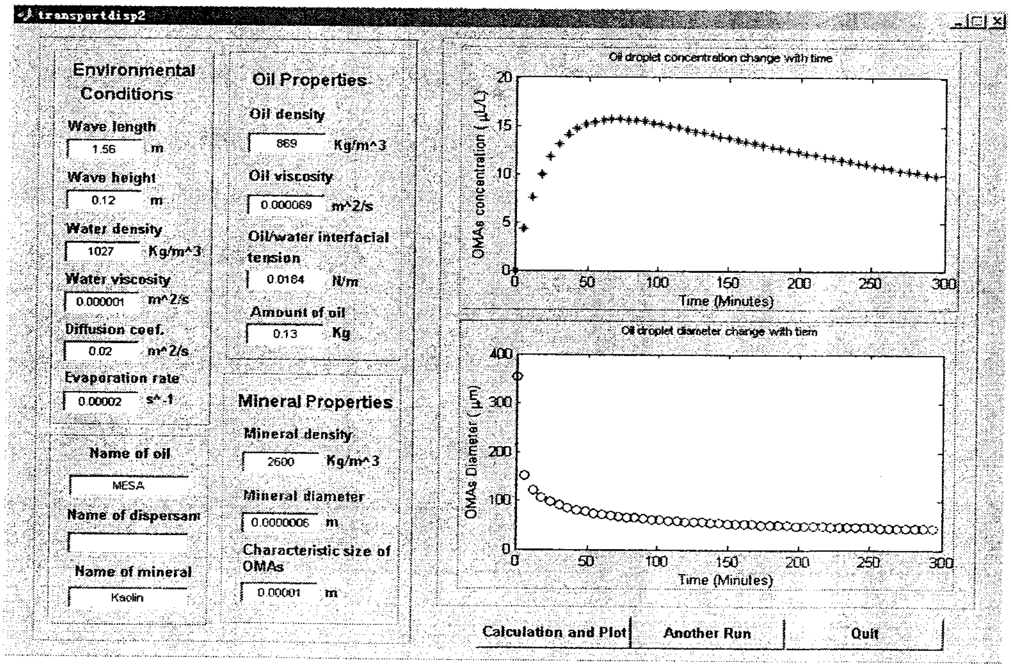

Environmental Conditions
Wave length 1.56 m
Wave height 0.12 m
Water density 1027 Kg/m^3
Water viscosity 0.000001 m^2/s
Diffusion coef. 0.02 m^2/s
Evaporation rate 0.00002 s^-1

Name of oil MESA
Name of dispersam
Name of mineral Kaolin

Oil Properties
Oil density 869 Kg/m^3
Oil viscosity 0.000069 m^2/s
Oil/water interfacial tension 0.0164 N/m
Amount of oil 0.13 Kg

Mineral Properties
Mineral density 2600 Kg/m^3
Mineral diameter 0.0000006 m
Characteristic size of OMAs 0.00001 m

Figure 5-5 Screen shot of the OMA-SIM user interface showing the input parameters and the modeling results of concentration and size of oil droplets and OMAs

Figure 5-6 presents the screen shot of the OMA-SIM user interface. It illustrates the input parameters and the histogram chart that is generated by the program for comparing the effect of wave energy dissipation rate on diameters of oil droplets.

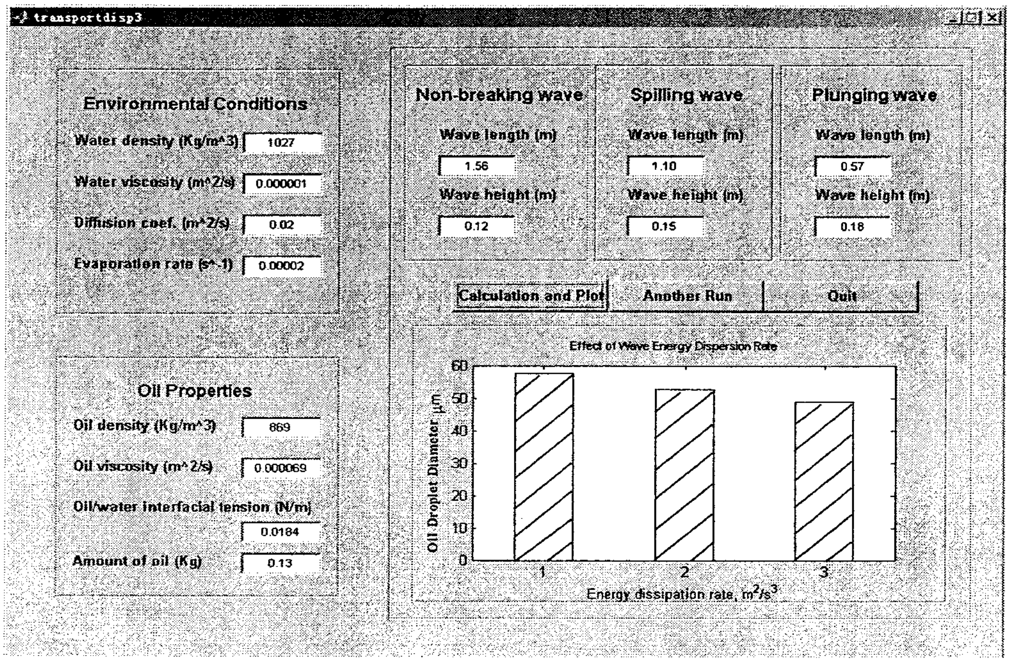

Water density (Kg/m^3) 1027
Water viscosity (m^2/s) 0.000001
Diffusion coef. (m^2/s) 0.02
Evaporation rate (s^-1) 0.00002

Oil density (Kg/m^3) 869
Oil viscosity (m^2/s) 0.000069
Oil/water interfacial tension (N/m) 0.0184
Amount of oil (Kg) 0.13

Non-breaking wave: Wave length (m) 1.56; Wave height (m) 0.12
Spilling wave: Wave length (m) 1.10; Wave height (m) 0.15
Plunging wave: Wave length (m) 0.57; Wave height (m) 0.18

Figure 5-6 Screen shot of the OMA-SIM user interface showing the input parameters and the modeling results of oil concentration under various wave conditions

The database mentioned previously contains three sub-databases: the oil properties database, mineral fines properties database, and dispersant properties database.

By clicking one of the database buttons, a corresponding Excel file containing the reference parameters is opened. After viewing the database data, the user then clicks the same database button to hide the Excel file.

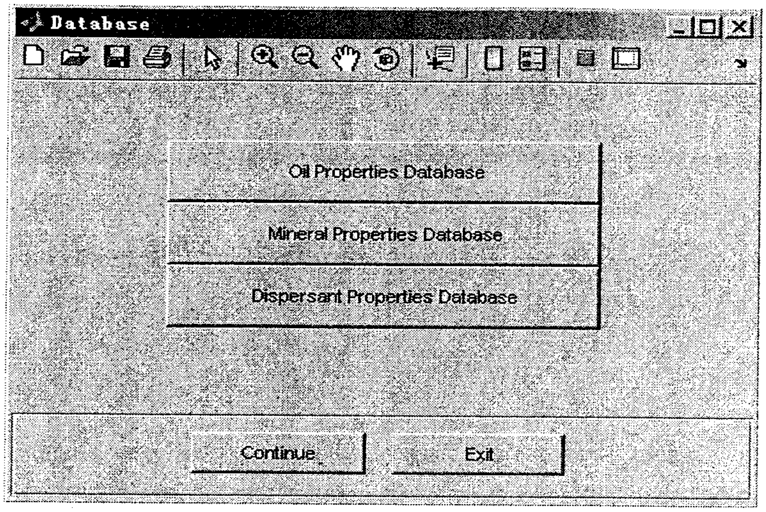

Figure 5-7 Screen shot of the OMA-SIM user interface database selection page

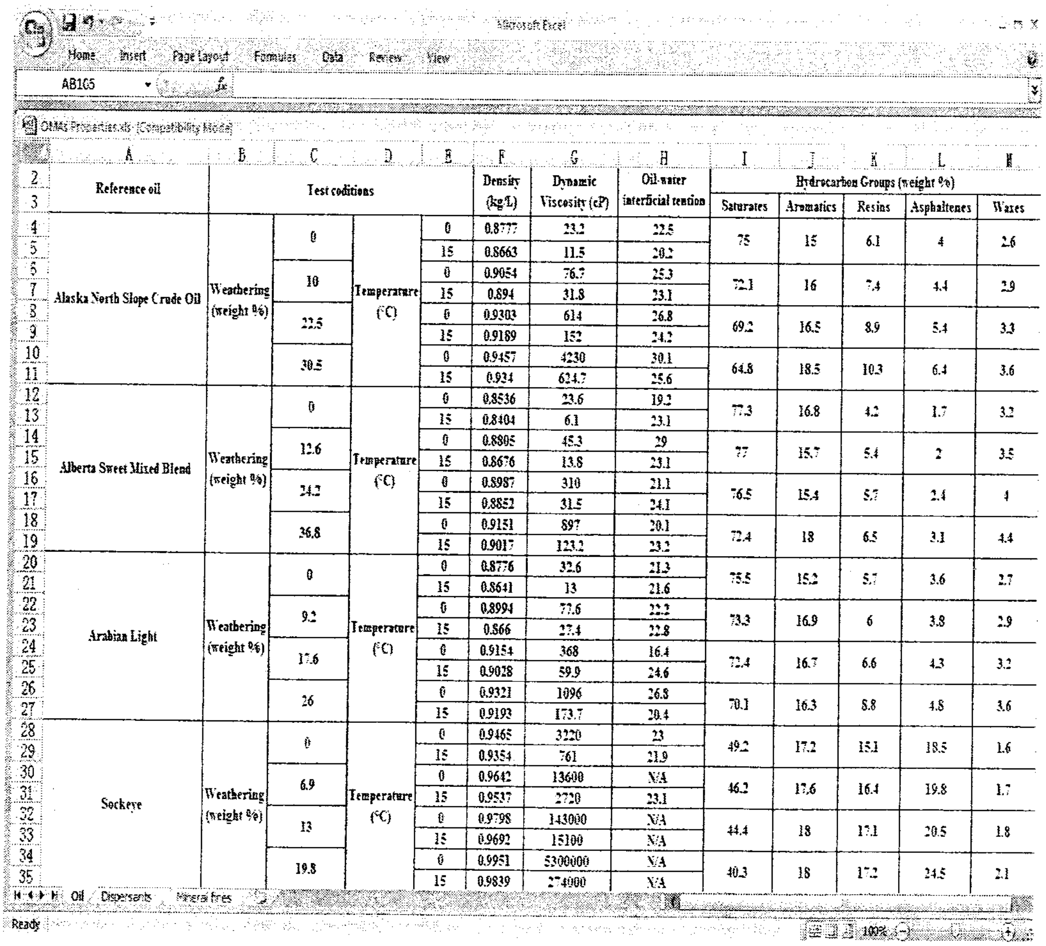

Reference oil	Test coditions				Density (kg/L)	Dynamic Viscosity (cP)	Oil-water interficial tention	Hydrocarbon Groups (weight %)				
								Saturates	Aromatics	Resins	Asphaltenes	Waxes
Alaska North Slope Crude Oil	Weathering (weight %)	0	Temperature (°C)	0	0.8777	23.2	22.5	75	15	6.1	4	2.6
				15	0.8663	11.5	20.2					
		10		0	0.9054	76.7	25.3	72.1	16	7.4	4.4	2.9
				15	0.894	31.8	23.1					
		22.5		0	0.9303	614	26.8	69.2	16.5	8.9	5.4	3.3
				15	0.9189	152	24.2					
		30.5		0	0.9457	4230	30.1	64.8	18.5	10.3	6.4	3.6
				15	0.934	624.7	25.6					
Alberta Sweet Mixed Blend	Weathering (weight %)	0	Temperature (°C)	0	0.8536	23.6	19.2	77.3	16.8	4.2	1.7	3.2
				15	0.8404	6.1	23.1					
		12.6		0	0.8805	45.3	29	77	15.7	5.4	2	3.5
				15	0.8676	13.8	23.1					
		24.2		0	0.8987	310	21.1	76.5	15.4	5.7	2.4	4
				15	0.8852	31.5	24.1					
		36.8		0	0.9151	897	20.1	72.4	18	6.5	3.1	4.4
				15	0.9017	123.2	23.2					
Arabian Light	Weathering (weight %)	0	Temperature (°C)	0	0.8776	32.6	21.3	75.5	15.2	5.7	3.6	2.7
				15	0.8641	13	21.6					
		9.2		0	0.8994	77.6	22.2	73.3	16.9	6	3.8	2.9
				15	0.866	27.4	22.8					
		17.6		0	0.9154	368	16.4	72.4	16.7	6.6	4.3	3.2
				15	0.9028	59.9	24.6					
		26		0	0.9321	1096	26.8	70.1	16.3	8.8	4.8	3.6
				15	0.9193	173.7	20.4					
Sockeye	Weathering (weight %)	0	Temperature (°C)	0	0.9465	3220	23	49.2	17.2	15.1	18.5	1.6
				15	0.9354	761	21.9					
		6.9		0	0.9642	13600	N/A	46.2	17.6	16.4	19.8	1.7
				15	0.9537	2720	23.1					
		13		0	0.9798	143000	N/A	44.4	18	17.1	20.5	1.8
				15	0.9692	15100	N/A					
		19.8		0	0.9951	5300000	N/A	40.3	18	17.2	24.5	2.1
				15	0.9839	274000	N/A					

Figure 5-8 Screen shot of the OMA-SIM user interface database showing the reference data from U.S. EPA (2003)

5.2 OMA-SIM Application Studies

A variety of interrelated factors contribute to the degree of oil vertical mixing and oil-mineral interactions that can lead to removal of spilled oil from the ocean and beaches. The principal functions of OMS-SIM were tested in four case studies to identify the parameters that are critical for both the formation and dispersion of oil/OMAs. The parameters studied include oil density, viscosity, oil/water interfacial tension, coupled with environmental conditions, such as temperature and water turbulence, which determine the extent of dispersed oil. Case Study 1 described in Section 5.2.1 attempts to simulate a beach environment, quantify the oil dispersion.

5.2.1 Case study 1: Effect of Oil Density and Viscosity

Density plays an important role in the fate of spilled oil since the density difference between oil and water ultimately determines the extent to which the slick is submerged and the residence time of oil droplets in the water column (National Research Council, 1985). Viscosity is a measure of a fluid's resistance to flow. It is important in terms of the degree of spreading of the oil and the formation of oil droplets, as this determines in part the surface area of oil available for attack by hydrocarbon-degrading microorganisms (Atlas and Bartha, 1992).

The effects of oil density and viscosity on the efficiency of spilled oil dispersion have been studied by experiments conducted with the Ohmsett wave tank (U.S. MMS, 2006). We used the same experimental parameters as input data for the OMA-SIM, in order to test if the model could simulate the effects of oil viscosity.

The Ohmsett wave tank used for the Case I experiments is the world's largest wave tank and is managed by the U.S. Minerals Management Service (U.S. MMS). The wave tank has the following dimension: 203 meters long, 20 meters wide, and 3.5 meters deep. It holds 10 million liters of seawater. A wave generator in the tank produces different wave types that simulate realistic sea environments.

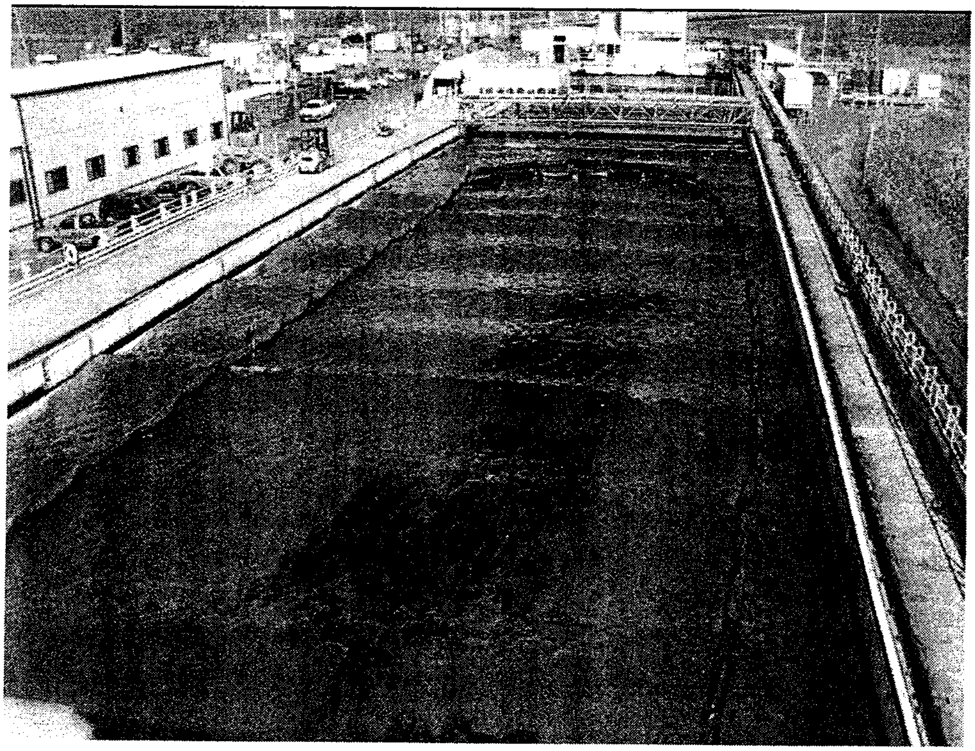

Figure 5-9 An oil slick dispersion experiment conducted with the Ohmsett wave tank (U.S. MMS, 2006)

At this experiment (U.S. MMS, 2006), the paddle frequency was set at 29 cpm to generate a wave frequency of 27.8 min^{-1} with a wave height of 0.33 m and wave length of 7.1 m. Three kinds of U.S. Outer Continental Shelf (OCS) oils were selected for the experiments. The density and viscosity of these oils are shown in Table 5-1.

Table 5-1 Summary of oils density and viscosity data used in the Ohmsett wave tank experiments (U.S. MMS, 2006)

Oil Type	Density (kg/m^3)	Viscosity (cP)
GA-209	852	14
IFO-30	937	252
EB-873	943	683

Figure 5-10 (a) shows the experimental data for oil concentration and oil droplet diameter obtained with GA-209 oil during 20 minutes of testing. The concentration of the GA-209 reached maximum value 5.2 ppm at the beginning of the test. Then the concentration gradually decreased to below 1 ppm. The diameter of the GA-209 droplets decreased from approximate 200 μm at the beginning to 50 μm at the end of the test.

Figure 5-20(b) presents the concentration values of IFO-30 oil decreased from 4.9 ppm to 1.3 ppm within two minutes of the test. Then the concentration is stable around 1.5 ppm. At the end of the test, the concentration increased gradually to 3 ppm. The diameter of the oil droplets ranged from 170 to 250 μm.

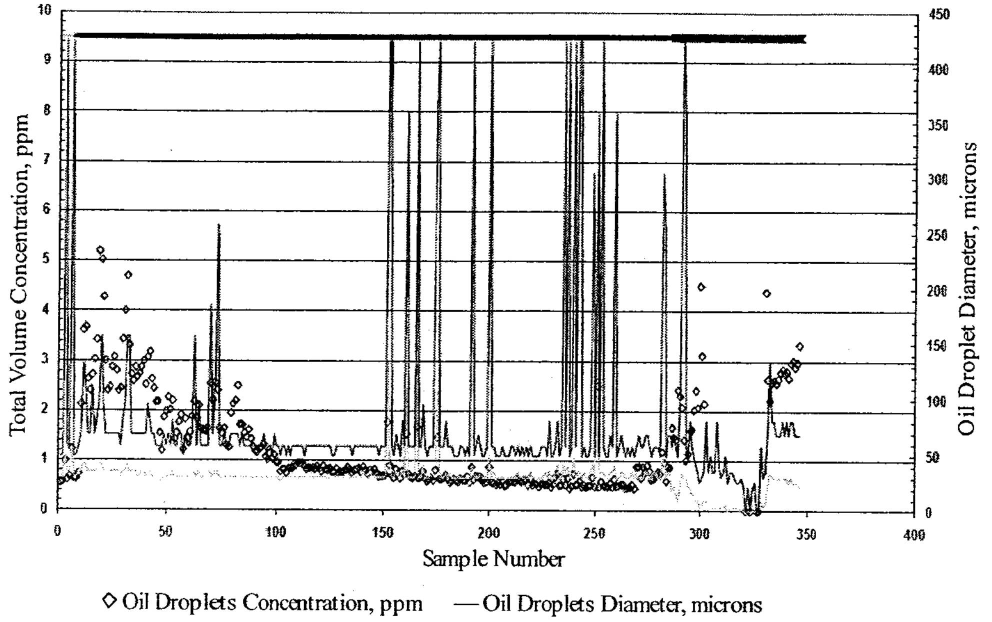

Figure 5-10(a) Experimental results for concentration and droplet size of GA-209 oil

(U.S. MMS, 2006)

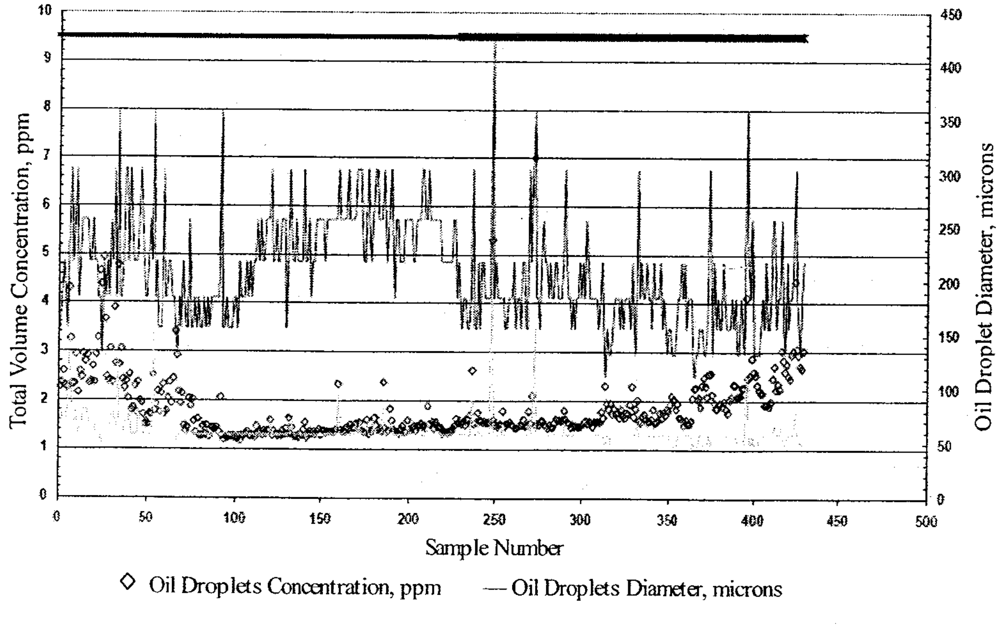

Figure 5-10(b) Experimental results for concentration and droplet size of IFO-30 oil

(U.S. MMS, 2006)

Figure 5-10(c) illustrates that the concentration values of EB-873 reaches 6.5 ppm at the beginning of the test. Then the concentration decreased to around 4 ppm. The diameter of the oil droplets decreased from 300 to 150μm.

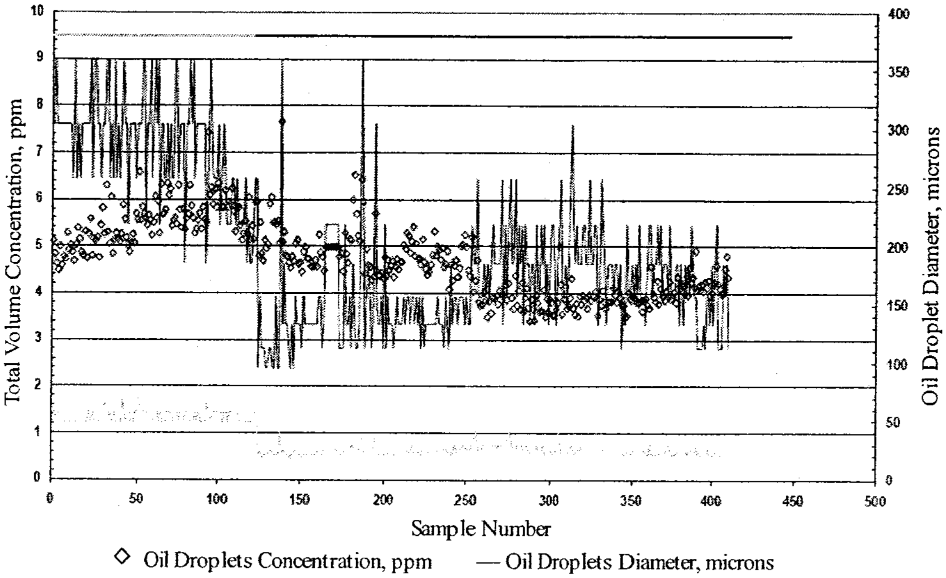

Figure 5-10(c) Experimental results for concentration and droplet size of EB-873 oil (U.S. MMS, 2006)

We used the experimental parameters obtained from Case study 1 as the input data for our OMA-SIM. Figure 5-11 presents the OMA-SIM results for the effect of oil viscosity on the oil concentration and oil droplet size in the mixing layer.

In the case of the high density, low viscosity GA-209 oil (curve comprised of stars), OMA-SIM simulated that the oil concentration reached a maximum value of 3.8 μL/L within first 2 minutes of the test (Figure 5-11, upper panel). The oil concentration curves for the oils with similar high density but higher viscosity (IFO-30 and EB-873) have the same shape as the GA-209 curve. Within 5 minutes, the peak oil concentration reached 6.5 and 7.2 μL/L for IFO 30 and EB 873 oils respectively. Based on our modeling results, the high density and high viscosity in EB-873 oil gave the highest oil concentration in seawater, whereas the low density and low viscosity of GA-209 oil gave the lowest oil concentration in seawater. Oil concentration of EB-873 is always higher than the values of the other two oils over the simulation.

Figure 5-11, lower panel, illustrates the effect of oil density and viscosity on oil droplet size. The oil droplets size decreased with time for all three types of oil due to wave action. From this figure, we observed the higher the viscosity of the oil, the larger the dispersed oil droplet size. The droplet size for low viscosity and low density of GA-209 oil decreases from 130 μm at the beginning to 70 μm after 20 minutes. The droplet size for high viscosity and high density of EB-873 oil ranges from 210 to 290 μm. This indicates that the droplet size of oil is directly proportional to oil viscosity. This simulation results agrees with the observation of Delvigne et al. (1987) and Huang and Elliot (1977). They observed the formation of larger oil droplets with increasing oil viscosity, which indicates that the viscosity of the oil influences the size of the oil droplets.

Experimental and simulation results indicate that density and viscosity are two of the major parameters that influence the formation of oil droplet and its dispersion. Furthermore, it will affect the ability of oil to form OMAs because larger oil droplets due to high oil viscosity is more preferential to buoy up to water surface than small oil droplets. Highly viscous oils will not form significant amount of OMAs, which has been reported by Lee et al. (1998), Bragg et al. (1994), and Wood et al. (1997). Stoffyn-Egli and Lee (2002) indicated that there is an inverse relationship between viscosity and OMA formation.

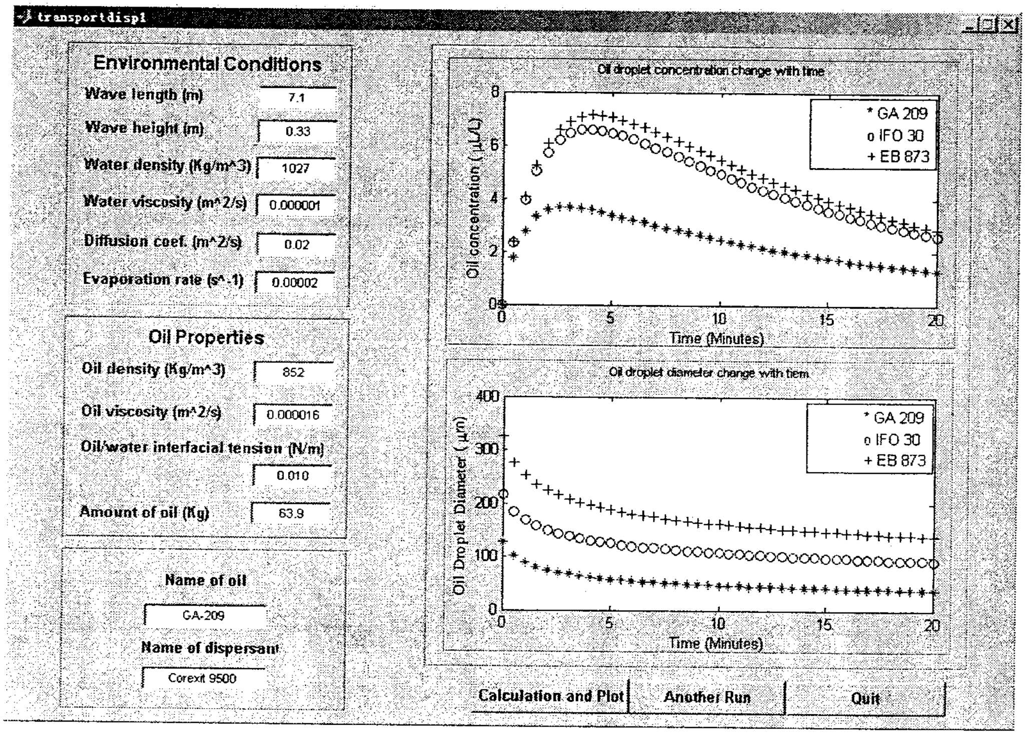

Environmental Conditions

Wave length (m) 7.1
Wave height (m) 0.33
Water density (Kg/m^3) 1027
Water viscosity (m^2/s) 0.000001
Diffusion coef. (m^2/s) 0.02
Evaporation rate (s^-1) 0.00002

Oil Properties

Oil density (Kg/m^3) 852
Oil viscosity (m^2/s) 0.000016
Oil/water interfacial tension (N/m) 0.010
Amount of oil (Kg) 63.9

Name of oil GA-209
Name of dispersant Corexit 9500

Figure 5-11 Screen shot of OMA-SIM results showing plots of oil droplet concentration with time (upper panel) and of oil droplet diameter with time (lower panel), for three different oils (GA 209, IFO 30, and EB 873), determining the effect of oil density and viscosity on oil dispersion

5.2.2 Case study 2: Effect of Oil-Water Interfacial Tension

Water-oil interfacial tension of crude oils is significantly reduced in the presence of dispersants such as Corexit 9500 and 9527. Khelifa et al. (2007)

conducted a dispersant test with Corexit 9500 that is illustrated in Figure 5-13. In his experiment, fresh oil (left side beaker) and an oil-dispersant mixture (right side beaker) were layered on the top of a 33% brine solution (Figure 5-12(a)) and then mixed vigorously (manually) for about one minute. As shown in Figure 5-12(b), the oil-dispersant mixture dispersed much easier than the oil alone. The water-oil interfacial tension was tested and for the oil was found to be 20 mN/m, and for oil-dispersants mixture was below 3.6 mN/m.

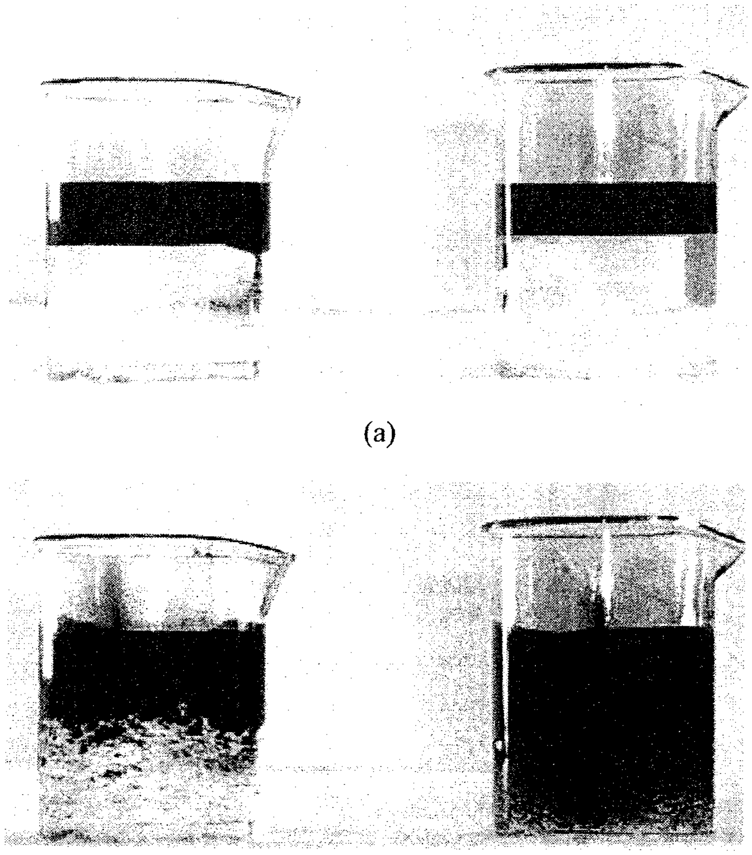

(a)

(b)

Figure 5-12 Dispersant testing: South Louisiana oil before (a) and after (b) 1 minute mixing with dispersant (In each of these pictures, the left beaker contains no dispersant and the right one has Corexit 9500 applied) (Khelifa et al., 2007)

A wave tank experiment on oil dispersion was carried out by Li et al. (2009). Fresh (unweathered) Alaska North Slope (ANS) oil was used to test the effectiveness of two dispersants, Corexit 9500 and SPC, assuming an ideal oil spill response scenario where dispersant application is available immediately after the incident. For the experiment, 300 ml of crude oil was gently poured onto the water surface within a 40 cm (inner diameter) ring located 10 m downstream from the wave maker, and 12 ml of dispersant was sprayed onto the surface of the oil slick through a pressurized nozzle. This resulted in a dispersant-to-oil ratio (DOR) of 1:25. The ring was then lifted prior to the first wave. Plunging breaking waves were produced with wave length of 2.16 m and wave height of 26 cm.

Figure 5-13 shows the experimental results of the dispersed ANS oil concentrations, as a function of time measured at a middle depth at a location downstream from the initial slick. The natural dispersed oil (without dispersant) concentration increased rapidly (within 5-10 min) and then decreased steadily. In the presence of dispersant, the oil concentration increased 3-6 fold comparing with the natural dispersed oil under breaking wave conditions.

The experimental parameters for this experiment were inputted into OMA-SIM using the same wave tank environmental conditions, to compare the effect of dispersant Corexit 9500 on the dispersed ANS oil concentration. The modeling results are illustrated in Figure 5-14.

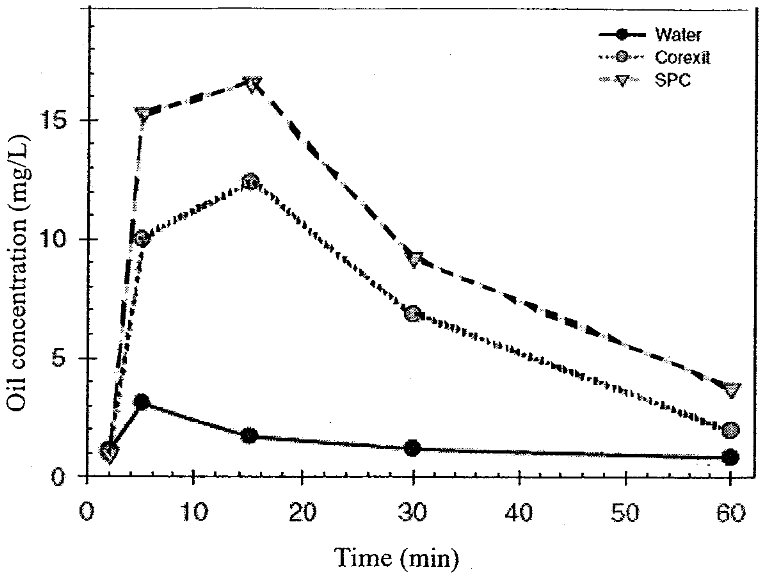

Figure 5-13 ANS oil concentration as a function of time in the wave tank in the presence and absence of two dispersants, Corexit 9500 and SPC (Li et al., 2009)

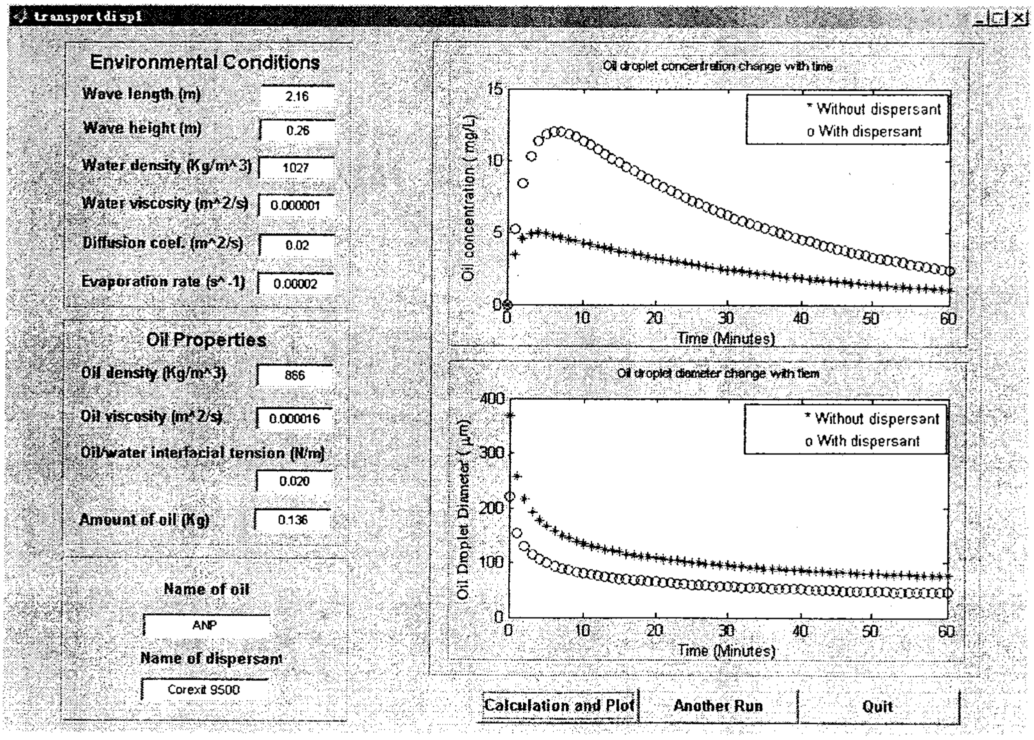

Environmental Conditions

Wave length (m) 2.16

Wave height (m) 0.26

Water density (Kg/m^3) 1027

Water viscosity (m^2/s) 0.000001

Diffusion coef. (m^2/s) 0.02

Evaporation rate (s^-1) 0.00002

Oil Properties

Oil density (Kg/m^3) 866

Oil viscosity (m^2/s) 0.000016

Oil/water interfacial tension (N/m) 0.020

Amount of oil (Kg) 0.136

Name of oil ANP

Name of dispersant Corexit 9500

Figure 5-14 Screen shot of the OMA-SIM user interface showing the input parameters and the modeling results for studying the effect of the dispersant Corexit 9500 on oil concentration and droplet diameter

Figure 5-14 (top panel) presents the OMA-SIM estimated concentration of ANS oil as a result of dispersion under breaking wave conditions. The application of Corexit 9500 significantly decreases oil/water interfacial tension (3.6 mN/m) and consequently increased oil concentration by 1.5 fold (circles), compared with oil alone (oil/water interfacial tension 20.2 mN/m; stars). These results are consistent with the experimental results of Khelifa et al. (2007). The lowering of interfacial tension in seawater caused by the dispersant helps to reduce the oil droplets size that enhances the spilled oil dispersion.

5.2.3 Case study 3: Effect of Temperature

The influence of temperature on the dispersion of oil/OMAs droplets is correlated with oil density, oil viscosity, and oil/water interfacial tension. Temperature is an important factor. It affects oil viscosity therefor influencing the rate of formation of OMAs. The viscosity of oil decreases with increasing temperature (Altas and Bartha, 1992; Walker and Colwell, 1974), and this facilitates to break up oil slicks at high temperatures (Devigne, 1987). Temperature also affects bacterial metabolism. In general, rates of oil degradation have been reported to decrease with decreasing temperatures due to depressed rates of enzymatic activity (Atlas and Bartha, 1992; Lee et al., 1997).

Table 5-2 shows reference data for properties of two different oils obtained from the U.S. EPA (2003). We selected ANS and West Texas Intermediate oils for study at 2 different temperatures (0°C and 15°C) using the OMA-SIM.

Table 5-2 Properties of ANS and WTI oils (U.S. EPA, 2003)

Reference oil	Temperature (°C)	Density (kg/L)	Dynamic Viscosity (cP)	Oil-water interficial tention (mN/m)
Alaska North Slope Crude Oil (ANS)	0	0.8777	23.2	22.5
	15	0.8663	11.5	20.2
West Texas Intermediate (WTI)	0	0.8594	19.2	18.8
	15	0.8474	8.6	15.6

Figure 5-15 presents a screen shot of the OMA-SIM simulation results for the estimated concentration and droplet diameter of the ANS and WTI oils at the two temperatures. For ANS (top right panel) under breaking wave conditions, the concentration in seawater at the end of the simulation period (300 min) was 2.4 μL/L at 0°C and it increased to 2.6μL/L at 15°C. WTI oil is less dense and less viscous than ANS oil. The concentrations of WTI oil at both 0°C and 15°C were higher than ANS. The concentration of dispersed WTI at 0°C was 2.7 μL/L and increased to 3.3 μL/L at 15°C. The modeling results indicated that oil concentration increases with temperature and decreases with oil density and viscosity.

Temperature affects the mean size of oil droplets slightly (low panel in Figure 5-15). For both ANS and WTI, the mean size at 0°C is larger than mean oil droplet size observed at 15°C. This is also observed in the experiment conducted by Khelifa et al. (2002).

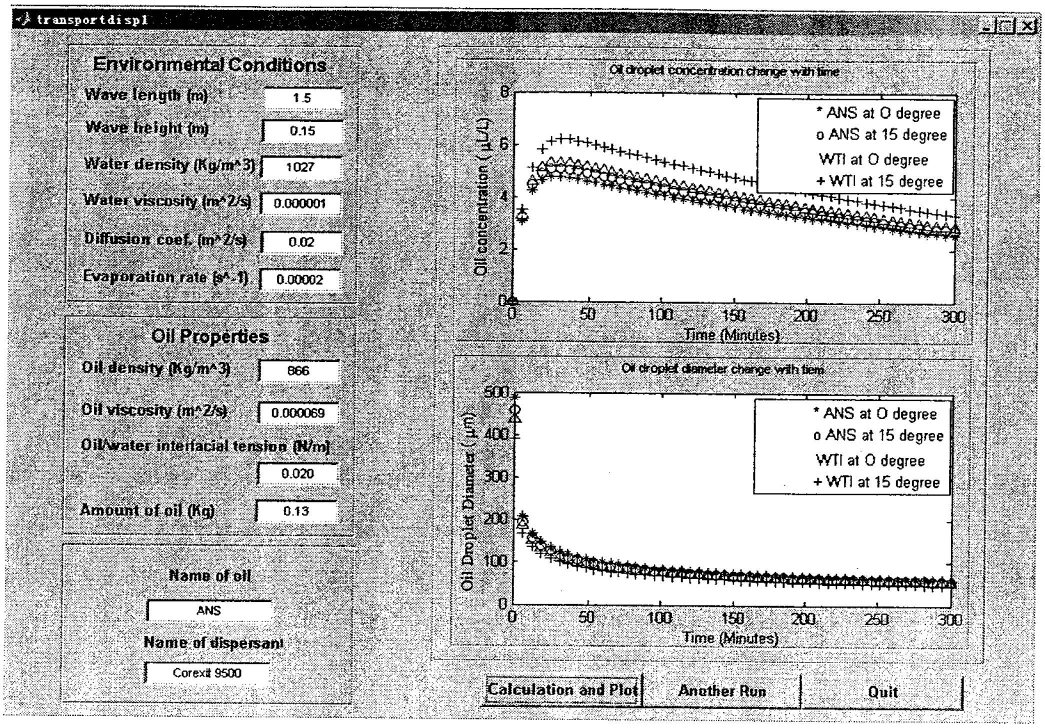

Environmental Conditions

Wave length (m) 1.5

Wave height (m) 0.15

Water density (Kg/m^3) 1027

Water viscosity (m^2/s) 0.000001

Diffusion coef. (m^2/s) 0.02

Evaporation rate (s^-1) 0.00002

Oil Properties

Oil density (Kg/m^3) 866

Oil viscosity (m^2/s) 0.000069

Oil/water interfacial tension (N/m) 0.020

Amount of oil (Kg) 0.13

Name of oil: ANS

Name of dispersant: Corexit 9500

Figure 5-15 Screen shot of the OMA-SIM user interface showing the input parameters and the modeling results for studying the effect of temperature on oil viscosity and then on oil dispersion

5.2.4 Case study 4: Effect of Wave Energy Dispersion Rate

Strong mixing due to turbulent wave energy is a necessary condition for OMAs formation and controls the size of the oil droplets by providing the shearing energy needed to break oil slicks into droplets (Delvigne, 1987). From the standpoint of oil spill mitigation, small oil droplets are preferred because they remain in suspension and are able to be dispersed with fewer tendencies to recoalesce. Big droplets will rise quickly to the water surface and coalesce, resisting dispersion. In order to generate small oil droplets, high dissipation energy rates are required.

An experiment was carried out by Li et al. (2009) for studying wave energy effects on oil dispersion. Two wave conditions, regular non-breaking waves and plunging breaking waves, were generated and their hydrodynamics characterized. The commercial chemical dispersant Corexit 9500, which is listed in the EPA oil spill contingency plan, was tested in the experiment. Crude oil Alaska North Slope with viscosity of 50.1 cP at 21°C was used in this test. Figure 5-16 illustrates the oil droplet diameter of the measured droplet size distribution changing with time (Li et al., 2009).

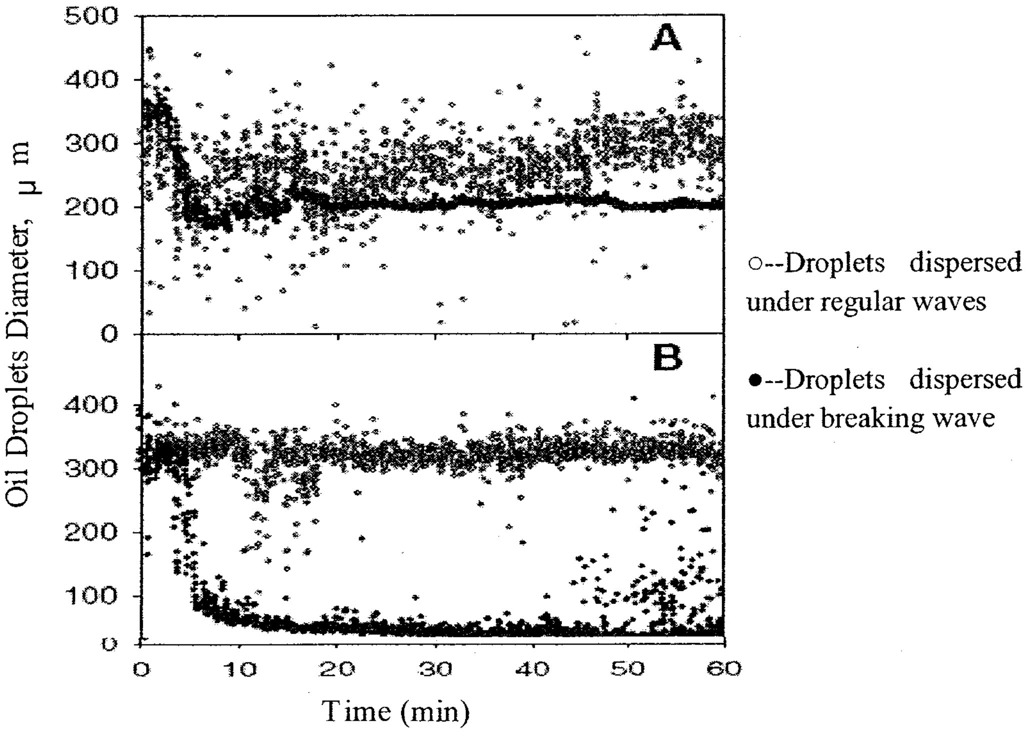

Figure 5-16 Dispersed ANS oil droplet size subjected to: (A) natural dispersion; (B) dispersion with Corexit 9500 applied (Li et al., 2009)

Applying the experimental parameters of Li et al. (2009) as the input data for the OMA-SIM, we simulate ANS oil dispersion under regular waves and breaking wave in natural dispersion (Figure 5-16 (A)) and in the presence of Corexit 9500 (Figure 5-16 (B)). The modeling results are illustrated in Figure 5-17.

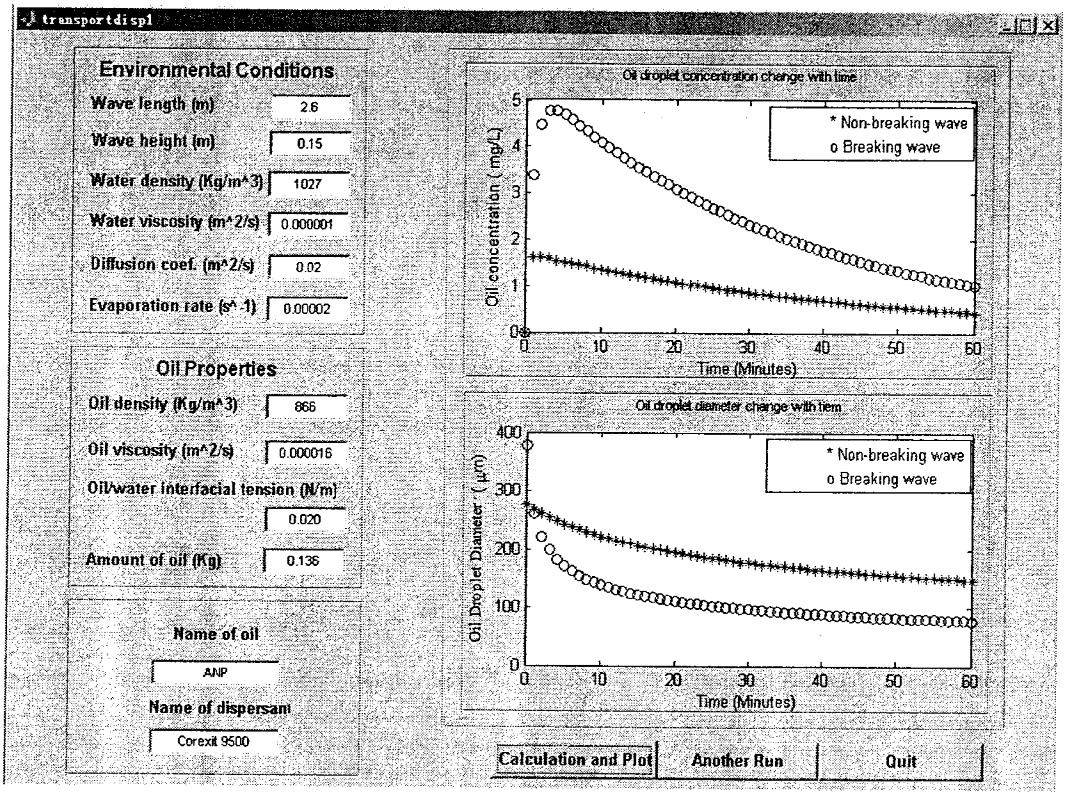
transportdispl

Environmental Conditions

Wave length (m) 2.6
Wave height (m) 0.15
Water density (Kg/m^3) 1027
Water viscosity (m^2/s) 0.000001
Diffusion coef. (m^2/s) 0.02
Evaporation rate (s^-1) 0.00002

Oil Properties

Oil density (Kg/m^3) 866
Oil viscosity (m^2/s) 0.000016
Oil/water interfacial tension (N/m) 0.020
Amount of oil (Kg) 0.136

Name of oil ANP
Name of dispersant Corexit 9500

Figure 5-17 Screen shot of the OMA-SIM user interface showing the input parameters and the modeling results for studying the effect of wave energy on oil dispersion rate

Figure 5-17 summarizes the OMA-SIM results of the effect of wave energy on the droplet size of the dispersed ANS oil. The modeling results of the droplet size of the dispersed oil agree well with the results of the experimental studies (Li et al., 2009).

The droplets started at the same oil droplet diameter level regardless of wave conditions. In the presence of the chemical dispersant Corexit 9500, the dispersed oil droplet sizes remained large but are considerably reduced in variability (oil droplet diameter 150~300 μm) under regular wave conditions; droplet sizes were dramatically reduced (oil droplet diameter ~100 μm) under breaking wave conditions within 10 min, and the oil droplet diameter continually decreased to about 50~80 μm under breaking wave conditions due to the high energy dissipation rate and turbulent diffusion.

5.3 Summary

In this chapter, a user-friendly interface was designed using Matlab and integrated with the OMA-SIM for simulating the formation of oil and OMA droplets and their dispersion after an oil spill. A user's guide was included to assist the operation of the software. The model system was applied to four experimental case studies. The OMA-SIM results were in agreement with the experimental results, suggesting that the model could provide a useful tool to simulate oil/OMAs dispersion.

Chapter 6

Thesis Contribution and Conclusion

6.1 Discussion

Numerical studies have significantly advanced the understanding of the mechanism of formation of the OMAs droplet (Lee et al., 1998, 2008; Lee and Stoffyn-Egli, 2001). This thesis research provides a new approach for modeling the formation of oil/OMAs and simulating their dispersion. Modeling results are validated against reported wave tank experiments. The main factors that affect oil/OMAs formation and vertical mixing were studied including the physical properties of oil and mineral fine under various environmental conditions (e.g. wave energy dissipation rate and temperature). Based on the studies mentioned in previous chapters, this thesis research provides the following findings:

1. The energy dissipation rate has a significant effect on the formation of oil droplets and OMAs. The dispersed oil under plunging breaker wave conditions is greater than that under regular non-breaker wave conditions. There is a good agreement between OMA-SIM results and what was observed in a wave tank experiment. (e.g. case studies in Chapter 4.1 and 5.2.4).
2. In the presence of mineral fines, the concentration of oil droplets and OMAs increased approximate 2 fold compared with that in the absence of mineral fines (e.g. case study in Chapter 4.2).
3. The size of oil droplets and OMAs in the presence of dispersant is 3 times higher than that absence of dispersant (e.g. case study in Chapter 4.2).
4. Oil viscosity, composition, and environmental temperature influence the formation and dispersion of oil droplets and OMAs. The trend of the curve obtained from the OMA-SIM simulation is similar to the curve obtained from published experiments. The oil viscosity decreases with increasing temperature. The more viscous the oil, the less oil and OMA droplets were dispersed into the water column (e.g. case studies in Chapter 5.2.1, 5.2.2, and 5.2.3).

It is reported that concentration and size of the mineral fines affect formation of OMAs (Ajijolaiya, 2004). Salinity and pH were also factors that influence the formation of OMAs (Lee et al., 2001; Lee, 2002). The effects of these factors will be determined in the future.

6.2 Conclusion

A brief summary of our conclusions based on applying the OMA-SIM are described as follows:

1. Oil viscosity has a significant influence on dispersed oil concentration. The mass of dispersed oil decreased with increasing oil viscosity.
2. Increasing temperature to decrease oil viscosity and then to enhance the formation of OMAs resulted in a greater concentration of oil.
3. OMA-SIM results indicated that the energy dissipation rate of breaking waves is the predominant factor which affects the concentration and particle size of oil droplets and OMAs. The higher the breaking wave energy, the more oil was dispersed with time after the experimental oil spill.
4. The effect of dispersants was to reduce oil/water interfacial tension and result in a decreased size of oil droplets and OMAs.
5. The application of mineral fines was to facilitate the formation of OMAs. It showed that mineral fines increased the concentration of suspended oil droplets and OMAs, and enhanced droplet stability.
6. The presence of dispersants and mineral fines enhanced the transfer of oil from the surface downward into the water by both increasing dispersed oil concentration and decreasing particle size of oil droplets.

6.3 Research Contribution

The research contribution is summarized as follows:

1. A new modeling approach (OMA-SIM) was developed in this study which consists of five modules. OMA-SIM couples an oil vertical mixing model with an oil droplets and mineral fines interaction model, and was used to simulate oil and OMAs formation and dispersion via vertical mixing in a near shore environment.
2. The main factors that affect oil droplets and OMAs formation and vertical mixing have been studied and considered in the developed model. These factors include oil density and viscosity, oil/water interfacial tension, wave energy dispersion rate, dispersants, and the size of mineral fines.
3. A graphical user-friendly interface written with Matlab code was constructed to run the model, together with an Excel spreadsheet containing useful reference data for the input parameters. A user guide was written to aid in the application of the model.

6.4 Recommendations for future studies

This thesis study presents OMA-SIM as an approach to study oil and OMA droplets formation and dispersion resulting from accidental oil spill and is designed for the management of near shore oil spills. Even though the simulation results are in agreement with the experimental results but it by no means completely addressed this challenging problem and therefore future research is required.

Based on the results obtained in the present study the following recommendation can be made:

1. Some mechanisms such as chemical reaction and biodegradation during oil dispersion should be taken into account in the future study.
2. Some factors that affect the formation and dispersion of oil/OMAs, such as concentration of mineral fines, shapes, salinity of the water were not concerned in this study. In a future study, these factors will be studied and integrated into the OMA-SIM.
3. In order to improve the accuracy of the model, we can integrate the stochastic analysis theory into our model to extend the model with the function of simulating the uncertainty generated during the experiments.
4. Application of mineral fines and dispersants, alone or in combination, has shown promising result in enhancing oil dispersion. Thus future work needs to be focused on the optimization of their types and concentration for treatment of near shore oil spills.
5. In order to enhance the effectiveness of the mineral fines and dispersants, optimization of the time and position of their addition to the oil plume needs to be performed in the future study.

The model developed for this study is designed to simulate oil and OMAs droplets vertical dispersion in water. Further work needs to be done to develop an integrated three-dimensional oil spill model that couples horizontal advection with vertical dispersion to address oil transport and fate with spatial and temporal variation.

REFERENCES

Ajijolaiya, L.O., 2004. The effects of mineral size and concentration on the formation of oil-mineral aggregates. M.A.S. thesis, Dept. of Civil and Resource Eng., Dalhousie University.

Atlas, R.M., and Bartha, R., 1992. Hydrocarbon biodegradation and oil spill bioremediation. In Advances in Microbial Ecology, Plenum Press, London. Vol 13, ed. K.C. Marshal , pp. 282–338.

Azetsu-Scott, K. and Johnson, B.D., 1992. Measuring Physical Characteristics of Particles: a New Method of Simultaneous Measurement for Size, Settling Velocity and Density of Constituent Matter. Deep Sea Res. 39(6), pp. 1057–1066.

Battjes, J.A. and Janssen, J.P.F.M., 1978. Energy loss and set-up due to breaking of random waves, Proc. 16th Coastal Engineering Conf., ASCE, pp.569–587.

Bassin, N. J., Ichiye, T., 1977. Flocculation behavior of suspended sediments and oil emulsions. Journal of Sedimentary Research. Vol. 47, pp. 671–677.

Belore R., 1985. Effectiveness of the Repeat Application of Chemical Dispersants on Oil. Environmental Studies Revolving Fund, Report No. 6, National Energy Board, Calgary, AB, pp. 30.

Belore, R., 2002. Wave Tank Tests to Determine the Effectiveness of Corexit 9500 Dispersant on Hibernia Crude Oil under Cold Water Conditions. In

Proceedings of the Twenty-fifth Arctic Marine Oil spill Program (AMOP) Technical Seminar, Environment Canada, Ottawa, ON, pp 735–740.

Binks, B.P., Lumsdon, S.O., 2000. Catastrophic phase inversion of water-in-oil emulsions stabilized by hydrophobic silica. Langmuir 16, pp. 2539–2547.

Boufadel, M.C., Bechtel, R.D., Weaver, J., 2006. The movement of oil under non-breaking waves. Marine Pollution Bulletin 52, pp. 1056–1065.

Bragg, J.R., Prince, R.C., Harner, E.J., Atlas, R.M., 1994. Effectiveness of Bioremediation for the Exxon Valdez oil spill. Nature 368, pp. 413–418.

Bragg, J.R., and Yang, S.H., 1995. Clay-oil flocculation and its effects on the rate of natural cleaning in Prince William Sound following the Exxon Valdez oil spill. Exxon Valdez Oil Spill - Fate and Effects in Alaskan Waters.American Society for Testing and Materials, Philadelphia, PA, pp. 178–214.

Brown, H.M., Goodman, R.H., and Canevari, G.P., 1985. Dispersant Effectiveness in Cold Water, in Proceedings of the Eighth Arctic Marine Oilspill Program (AMOP) Technical Seminar, Environment Canada, Ottawa, ON, pp. 245–259.

Cloutier, D., Amos, C.L., Hill, P.R., and Lee, K., 2002. Oil erosion in an annular flume by seawater of varying turbidities: A critical bed shear stress approach. Spill Science & Technology Bulletin 8(1), pp. 83–93.

Dantas, T.N.D., Neto, A.A.D., Moura, E.F., 2001. Microemulsion systems applied to breakdown petroleum emulsions. Journal of Petroleum Science and Engineering 32 (2-4), pp. 145–149.

Davis, J.T., 1985. Drop sizes of emulsions related to turbulent energy dissipation rates. Chemical Engineering Science 40(5): pp. 839–842.

Delvigne, G.A.L., 1987. Droplet size distribution of naturally dispersed oil: In Kuiper, J. and Van den Brink, W.J., eds., Fate and effects of oil in marine ecosystems, Martinus Nighoff Publications, Dordrecht, Netherlands, pp. 29–40.

Delvigne, G.A.L., and Sweeney, C.E., 1988. Natural dispersion of oil, Oil and Chemical Pollution 4, pp. 281–310.

Edelvang, K., Larsen, M., 1995. The flocculation of fine-grained sediment in the estuary of Ho Bugt, Denmark. - Folia geogr, dan. 22, pp. 1–120.

Elliott, A.J., 1986. Shear diffusion and the spread of oil in the surface layers of the North Sea. Deutsche Hydrographische Zeitschrift 39, pp. 113–137.

U.S. Environmental Protection Agency (U.S. EPA), 2003. Characteristics of Spilled Oils, Fuels, and Petroleum Products: 1. Composition and Properties of Selected Oils, National Exposure Research Laboratory, U.S. EPA publication, EPA/600/R–03/02.

Fay, J.A., 1969. The spread of oil slick on a calm sea. In: Hoult, D.P. (Ed.), Oil on the Sea. Plenum Press, New York, NY, pp. 53–63.

Fraser, J.P., Wicks, M., 1995. Estimation of maximum stable oil droplet sizes at sea resulting from natural dispersion and from use of a dispersant. In: Proceedings of the 18th Arctic and Marine Oil Spill Program (AMOP), Technical Seminar, pp. 313–316.

Graf, W.H., 1971. Hydraulics of Sediment Transport. McGraw-Hill, NewYork.

Guyomarch, J., Merlin, F.X., Bernanose, P., 1999. Oil interaction with mineral fines and chemical dispersion: Behaviour of the dispersed oil in coastal or estuarine conditions. In: Proceedings of the 22nd Arctic and Marine Oil Spill Program (AMOP), Technical Seminar, Calgary, Alberta, Canada, pp. 137–149.

Guyomarch, J., Le Floch, S., Merlin, F.X., 2002. Effect of suspended mineral load, water salinity and oil type on the size of oil–mineral aggregates in the presence of chemical dispersant, Spill Science & Technology Bulletin 8 (1), pp. 95–100.

Hasselmann, K., 1974. On spectral dissipation of ocean waves due to white capping. Boundary-Layer Meteorology 6, pp. 107–127.

Hawley, N., 1982. Settling Velocity Distribution of Natural Aggregates. Journal of Geophysical Research. 87(C12), pp. 9489–9498.

Hill, P.S., Nowell, A.R.M., 1995. Comparison of two models of aggregation in continental-shelf bottom boundary layers. Journal of Geophysical Research 100 (C11), pp. 22,749–22,763.

Hill, P.S., Khelifa, A., Lee, K., 2002. Time-scale for oil droplet stabilization by mineral particles in turbulent suspensions. Spill Science & Technology Bulletin 8 (1), pp. 73–81.

Hinze, J.O., 1995. Fundamentals of the hydrodynamic mechanism of splitting in dispersion processes. Journal of AICHE 1, pp. 289–295.

Huang, C.P., and Elliott, H.A., 1977. The stability of emulsified crude oils as affected by suspended particles: In Wolfe, D.A., ed., Fate and effect of petroleum hydrocarbon on marine organisms and ecosystem, Pergamon Press, pp. 412–420.

Huang, J.C., 1983. A review of the state-of-the-art of oil spill fate behaviour models. In: Proceedings of the 1983 Oil Spill Conference, API, Washington DC, pp. 313–322.

Ives, K. J., 1978. The Scientific Basis of Flocculation, Sijthoff & Noordhoff. Alohen aan den Rijn.

Jackson, G.A., 1998. Using Fractal Scaling and Two Dimensional Particle Size Spectra to Calculate Coagulation Rates for Heterogeneous Systems. Journal of Colloid Interface Science. 202, pp. 20–29.

Johansen, O., 1982. Dispersion of oil from drifting slicks. Spill Technology Newsletter, pp. 134–149.

Johnson, B., 1997. International Towing Tank Conference: ITTC Symbols and Terminology List, U.S. Naval Academy, Annapolis, MD.

Khelifa, A., Egli, P., Hill, P.S., Lee, K., 2002. Characteristics of oil droplets stabilized by mineral particles: effects of oil type and temperature. Spill Science & Technology Bulletin 8 (1), pp. 19–30.

Tkalich, P., Chan, E.S., 2003. The third-order polynomial method for two-dimensional convection and diffusion. International Journal for Numerical Methods in Fluids 41 (9), pp. 997–1019.

Khelifa, A., Fingas, M.F., Hollebone, B.P., Brown, C.E., 2007. Effects of Chemical Dispersants on Oil Physical Properties and Dispersion, in Proceedings of the Thirtieth Arctic and Marine Oil Spill Program Technical Seminar, Environment Canada, Ottawa, Ontario, pp. 105–116.

Kranenburg, C., 1994. The Fractal Structure of Cohesive Sediment Aggregates. Estuarine Coastal Shelf Science. 39, pp. 451–460.

Lamarre, E., Melville, W.K., 1991. Air entrainment and dissipation in breaking waves. Nature 351, pp. 469–472.

Lambert, P., Fieldhouse, B., Wang, Z., Fingas, M., Goldthorp, M., Pearson L., and Collazzi, E., 2001. A Laboratory Study of Flow-through Fluorometer for Measuring Oil-in-Water Levels, in Proceedings of the Twenty-fourth Arctic and Marine Oil Spill Program (AMOP) Technical Seminar, Environment Canada, Ottawa, ON, pp 23–45.

Lau,Y.L. and Krishnappan, B.G., 1997. Measurement of Size Distribution of Settling Flocs. NWRI Publication No. 97-223, National Water Research Institute, Environment Canada, CCIW, Burlington, Ontario, Canada.

Lee, D.G., Bonner, J.S., Garton, L.S., Ernest, A.N.S., Autenrieth, R.L., 2002. Modeling coagulation kinetics incorporating fractal theories: comparison with observed data. Water Research. 36 (4), pp. 1056–1066.

Lee, K., Weise, A. M., and St-Pierre, S., 1996. Enhanced oil biodegradation with mineral fine interaction. Spill Science & Technology Bulletin 54(7), pp. 983–993.

Lee, K., Lunel, T., Wood, P., Swannell, R., Stoffyn-Egli, P., 1997. Shoreline cleanup by acceleration of clay-oil flocculation processes. In: Proceedings of 1997 International Oil Spill Conference. American Petroleum Institute, Washington, DC, pp. 235–240.

Lee, K., Stoffyn-Egli, P., Wood, P.A., Lunel, T., 1998. Formation and Structure of Oil-Mineral Fines Aggregates in Coastal Environments. In: Proceedings of the 21st Arctic and Marine Oilspill Program (AMOP) Technical Seminar, Ottawa, Ont., pp. 911–921.

Lee, K., Stoffyn-Egli, P., 2001. Characterization of Oil-Mineral Aggregates. In: Proceedings of the 2001 International Oil Spill Conference, American Petroleum Institute, Korea, pp. 991–996.

Lee, K., 2002. Oil-particle interactions in aquatic environments: influence on the transport, fate, effect and remediation of oil spills. Spill Science & Technology Bulletin 8 (1), pp. 3–8.

Lee, K., Stoffyn-Egli, P., Tremblay, G. H., Owens, E. H., Sergy, G. A., Guenette, C. C., Prince, R. C., 2003. Oil-mineral aggregate formation on oiled beaches:

Natural attenuation and sediment relocation. Spill Science & Technology Bulletin, 8(3), pp. 285–296.

Lee, K., Li, Z., King, T., Kepkay, P., Boufadel, M. C., Venosa, A. D., Mullin, J. V., 2008. Effects of chemical dispersants and mineral fines on partitioning of petroleum hydrocarbons in natural seawater. International Oil Spill Conference, pp.633–638.

Leonard, B.P., 1979. A stable and accurate convective modeling procedure based on quadratic upstream interpolation. Computer Methods in Applied Mechanics and Engineering 19, pp. 59–98.

Leonard, B.P., MacVean, M.K., Lock, A.P., 1995. The flux integral method for multidimensional advection and diffusion. Applied Mathematical Modelling 19, pp. 333–342.

Lessard, R.R., Demarco, G., 2000. The significance of oil spill dispersants. Spill Science & Technology Bulletin 6 (1), pp. 59–68.

Li, D.H., Ganczarczyk, J., 1989. Fractal geometry of particle aggregates generated in water and wastewater treatment processes. Environmental Science and Technology. 23, pp. 1385–1389.

Li, M., and Garrett, C., 1998. The Relationship Between Oil Droplet Size and Upper Ocean Turbulence, Marine Pollution Bulletin, Vol. 36, No. 12, pp. 961–970.

Li, Z., Kepkay, P., Lee, K., King, T., Boufadel, M.C., Venosa, A.D., 2007. Effects of chemical dispersants and mineral fines on crude oil dispersion in a wave tank under breaking waves. Marine Pollution Bulletin 54, pp. 983–993.

Li, Z., Lee, K., King, T., Boufadel, M.C., Venosa, A.D., 2008. Oil droplet distribution as a function of energy dissipation rate in an experimental wave tank. International Oil Spill Conference, pp. 621–626.

Li, Z., Lee, K., King, T., Boufadel, M.C., Venosa, A.D., 2009. Evaluating crude oil chemical dispersion efficacy in a flow-through wave tank under regular non-breaking wave and breaking wave conditions. Marine Pollution Bulletin 58, 735–744.

Lunel, T., 1995. Understanding the mechanism of dispersion through oil droplet size measurements at sea. In: Lane, P. (Ed.), The Use of Chemicals in Oil Spill Response. ASTM STP 1252. American Society for Testing and Materials, Philadelphia, PA, pp. 240–270.

Lunel, T., Swannell, R., Rusin, J., 1997. Monitoring the effectiveness of response operations during the Sea Empress incident: a key component of the successful. Oceanographic Literature Review 44(12), pp. 1570–1570.

Ma, X., Cogswell, A., Li, Z., Lee, K., 2007. Particle size analysis of dispersed oil and oil-mineral aggregates with an automated ultraviolet Epi-fluorescence microscopy system. Environmental Technology, Vol. 29, pp. 739–748.

Mackay, D., Buist, I., Mascarenhas, R., Paterson, S., 1980. Oil Spill Processes and Models, Report EE8. Environment Canada, Ottawa.

Mackay, D., Hussain, K., 1982. An exploratory study of sedimentation of naturally and chemically-dispersed oil. Environment Canada Report, EE-35, Ottawa, Ontario, Canada, pp. 24.

Marczewski, A.W., Szymula, M., 2002. Adsorption of asphaltenes from toluene on mineral surface. Colloids and Surfaces A-Physicochemical and Engineering Aspects 208 (1–3), pp. 259–266.

McCave, I.N., 1984. Size Spectra and Aggregation of Suspended Particles in the Deep Ocean. Deep Sea Research. 31(4), pp. 329–352.

Menon, V.B., Wasan, D.T., 1986. Particle-fluid interactions with application to solid-stabilized emulsions. Part I. The effect of asphaltene adsorption. Colloids and Surfaces 19, pp. 89–105.

Meyers P.A., Quinn J.G., 1973. Factors affecting the association of fatty acids with mineral particles in sea water. Geochim Cosmochim Acta 37, pp. 1745–1759.

U.S. Minerals Management Service (U.S. MMS), 2006. Chemical dispersibility of U.S. Outer Continental Shelf Crude Oils in Non-Breaking Waves. Herndon, VA.

Mullin, J.V.,Lane, J.A., 2000. Users Guide to the OHMSETT Oil Spill Response Test Facility, Spill Science and Technology, Vol. 6, pp. 77–87.

Muschenheim, D. K., Lee, K., 2002. Removal of oil from the sea surface through particulate interactions: Review and prospectus. Spill Science & Technology Bulletin, 5(3-4), pp. 177–289.

National Research Council (NRC), 1985. Oil in the sea: Inputs, Fates, and Effects. National Academy Press, Washington DC, pp. 601.

Nihoul, J.C.L., 1983. A non-linear mathematical model for the transport and spreading of oil slicks. Ecological Modelling, pp. 325–339.

Omotoso, O. E., Munoz, V. A., Mikula, R. J., 2002. Mechanisms of crude oil-mineral interactions. Spill Science & Technology Bulletin 8(1), pp. 45–54.

Owens, E.H., Bragg, J.R., Humphrey, B., 1994. Clay-oil flocculation as a natural cleansing process following oil spills: Part 2-Implications of study results in understanding past spills and for future response decisions. In: Proceedings 17th Arctic and Marine Oil Spill Program (AMOP) Technical Seminar, Edmonton, Alberta, pp. 25–37.

Owens, E.H., 1998. Sediment relocation and tilling-underused and misunderstood techniques for the treatment of oiled beaches. In: Proceedings of 21st Arctic and Marine Oilspill Program (AMOP) Technical Seminar. Environment Canada, Ottawa, ON, pp. 857–872.

Owens, E. H., Lee, K., 2003. Interaction of oil and mineral fines on shorelines: review and assessment. Marine Pollution Bulletin, 47(9-12), pp. 397-405.

Owens, E.H., Sergy, G.A., Guenette, C.C., Prince, R.C., Lee, K., 2003. The reduction of stranded oil by in situ shoreline treatment options. Spill Science & Technology Bulletin 8 (3), pp. 257–272.

Owens, E.H., 1999. The interaction of fine particles with stranded oil. Pure and Applied Chemistry 71 (1), pp. 83–93.

Page, C., P. Sumner, R. Autenrieth, J. Bonner and T. McDonald, 1998. Hydrodynamic Characterization of the COSS (Coastal Oil Spill Simulation System), in Proceedings of the Twenty-first Arctic and Marine Oil spill Program (AMOP) Technical Seminar, Environment Canada, Ottawa, ON, pp. 89–99.

Page, C., Sumner, P., Autenrieth, R., Bonner, J., and McDonald, T., 1999. Materials Balance on a Chemically-Dispersed Oil and a Whole Oil Exposed to an Experimental Beach Front, in Proceedings of the Twenty-second Arctic and Marine Oil spill Program (AMOP) Technical Seminar, Environment Canada, Ottawa, ON, pp. 645–658.

Page, D. S., Boehm, P. D., Brown, J. S., Neff, J. M., Burns, W. A., Bence, A. E., 2005. Mussels document loss of bioavailable polycyclic aromatic hydrocarbons and the return to baseline conditions for oiled shorelines in Prince William Sound, Alaska. Marine Environmental Research, 60(4), pp. 422–436.

Raj, P.P.K. 1977. Theoretical study to determine the sea state limit for the survival of oil slicks on the ocean, Report CG-D-90-77. U.S. Coast Guard, Washington DC, USA.

Rattanapitikon, W. and Shibayama, T., 1998. Energy Dissipation Model for Irregular Breaking Waves, Proceedings of the 26th Coastal Engineering Conf., ASCE, pp.112–125.

Reed, M., Johansen, O., Brandvik, P.J., Daling, P., Lewis, A., Fiocco, R., Mackay, D., Prentki, R., 1999. Oil spill modeling toward the close of the 20th century:

overview of the state of the art. Spill Science and Technology Bulletin 5 (1), pp. 3–16.

Reilly, T.J., Kraus, N.C., Wise, W.R., R. Jamail, R. 1994. COSS: A Mesoscale Test Spill Research, Spill Science and Technology, Vol. 1, pp. 165–167.

Ross, S., Buist, I., Potter, S., Belore, R., and Lewis, A., 2001. Dispersant Testing of OHMSETT: Feasibility Study and Preliminary Testing, in Proceedings of the 2001 International Oil Spill Conference, American Petroleum Institute, Washington, DC, pp. 461–466.

SAIC, 2003. Process for the Removal of Spent Oil Spill Dispersants from Test Water at the National Oil Spill Response Test Facility, Report for the United States Department of the Interior, Minerals Management Service, Herndon, VA, pp. 37.

Sergy, G., Guennette, C., Owens, E., Prince, R., and Lee, K., 1999. Treatment of oiled sediment shorelines by sediment relocation. In: Proceedings of the 1999 International Oil Spill Conference, Seattle, Washington, USA, pp. 549–554.

Shaw, J.M., 2003. A Microscopic View of Oil Slick Break-up and Emulsion Formation in Breaking Waves. Spill Science & Technology Bulletin, 8(5–6), pp. 491–501.

Southgate, H.N., Nairn, R.B., 1993. Deterministic profile modeling of nearshore processes. Part 1. Wave and currents, Coastal Engineering, Vol.19, pp.27–56.

Spaulding, M.L., Howlett, E., Anderson, E., and Jayko, K., 1992. OILMAP: a global approach to spill modeling. Proceedings of the 15th Arctic and Marine Oil Spill Program Technical Seminar. Environment Canada, pp. 15–21.

Sterling, M.C., Bonner, J.S., Ernest, A.N.S., Page, C.A., and Autenrieth, R.L., 2005. Application of fractal flocculation and vertical transport model to aquatic sol-sediment systems, Water Research 39 (9), pp. 1818–1830.

Stoffyn-Egli, P., Lee, K., 2002. Formation and characterization of oil - mineral aggregates. Spill Science and Technology Bulletin, Vol. 8, pp. 31–44.

Stozenbach, K.D., Madsen, O.S., Adams, E.E., Pollack, A.M., and Cooper C.K., 1977. A Review and Evaluation of Basic Techniques for Predicting the Behavior of Surface Oil Slicks. Report No. 222. R.M. Parsons Laboratory for Water Resources and Hydrodynamics, Report No. 222, MIT, Cambridge, MA.

Szymula, M., Marczewski, A.W., 2002. Adsorption of asphaltenes from toluene on typical soils of Lublin region. Applied Surface Science 196 (1-4), pp. 301–311.

Tambo, N., Watanabe,Y., 1979. Physical Aspect of Flocculation Process—I. Fundamental Treatise. Water Research. 13, pp. 429–439.

Tkalich, P., and Chan, E.S., 2002. Vertical mixing of oil droplets by breaking waves. Marine Pollution Bulletin 44 (11), pp. 1219–1229.

Tkalich, P., 2006. A CFD solution of oil spill problems. Environmental Modelling & Software, Vol. 21, Issue 2, pp. 271–282.

Van Leussen, W., 1988. Aggregation of Particles, Settling Velocity of Mud Flocs: a Review. In: Dronkers, J. and van Leussen, W. (eds) Physical Processes in Estuaries, Springer-Verlag, NewYork, pp. 347–403.

Venosa, A. D., Lee, K., Boufadel, M. C., Li, Z., Olsen, E. W., King, T., 2008. Dispersant effectiveness as a function of energy dissipation rate in an experimental wave tank, International Oil Spill Conference, pp. 777–784.

Whitby, C. P., Fornasiero, D., Ralston, J., 2008. Effect of oil soluble surfactant in emulsions stabilized by clay particles. J. Colloid Interface Science. 323, pp. 410–419.

Winterwerp, J.C., 1998. A Simple Model for Turbulence Induced Flocculation of Cohesive Sediment. Journal of Hydraulic Research. 36(3), pp. 309–326.

Wood, P., Lunel, T., Bailey, N., Lee, K., Stoffyn-Egli, P., 1997. Clay-oil flocculation during surf washing at the Sea Empress incident. In: Proceedings of 20th Arctic and Marine Oil spill Program (AMOP) Technical Seminar. Environment Canada, Ottawa, ON, pp. 1085–1105.